Title
Black carbon aerosol dynamics and isotopic composition in Alaska linked with boreal fire emissions and depth of burn in organic soils

Journal
Global Biogeochemical Cycles, 29(11)

ISSN
0886-6236

Authors
Mouteva, GO
Czimczik, CI
Fahrni, SM
et al.

Publication Date
2015-11-01

DOI
10.1002/2015gb005247

Peer reviewed

AGU PUBLICATIONS

Global Biogeochemical Cycles

RESEARCH ARTICLE
10.1002/2015GB005247

Key Points:
- Boreal fire was the dominant contributor to aerosol variability during summer
- The radiocarbon content of fire aerosol was higher than many prior estimates
- Aerosol and soil isotopes together may constrain regionwide depth of burn

Correspondence to:
G. O. Mouteva,
gmouteva@uci.edu

Citation:
Mouteva, G. O., et al. (2015), Black carbon aerosol dynamics and isotopic composition in Alaska linked with boreal fire emissions and depth of burn in organic soils, *Global Biogeochem. Cycles*, *29*, doi:10.1002/2015GB005247.

Received 22 JUL 2015
Accepted 5 OCT 2015
Accepted article online 8 OCT 2015

Black carbon aerosol dynamics and isotopic composition in Alaska linked with boreal fire emissions and depth of burn in organic soils

G. O. Mouteva[1], C. I. Czimczik[1], S. M. Fahrni[1,2], E. B. Wiggins[1], B. M. Rogers[3], S. Veraverbeke[1], X. Xu[1], G. M. Santos[1], J. Henderson[4], C. E. Miller[5], and J. T. Randerson[1]

[1]Department of Earth System Science, University of California, Irvine, California, USA, [2]Now at Eidgenössische Technische Hochschule, Zürich, Switzerland, [3]Woods Hole Research Center, Falmouth, Massachusetts, USA, [4]Atmospheric and Environmental Research, Inc., Lexington, Massachusetts, USA, [5]Jet Propulsion Laboratory, California Institute of Technology, Pasadena, California, USA

Abstract Black carbon (BC) aerosol emitted by boreal fires has the potential to accelerate losses of snow and ice in many areas of the Arctic, yet the importance of this source relative to fossil fuel BC emissions from lower latitudes remains uncertain. Here we present measurements of the isotopic composition of BC and organic carbon (OC) aerosols collected at two locations in interior Alaska during the summer of 2013, as part of NASA's Carbon in Arctic Reservoirs Vulnerability Experiment. We isolated BC from fine air particulate matter ($PM_{2.5}$) and measured its radiocarbon ($\Delta^{14}C$) content with accelerator mass spectrometry. We show that fires were the dominant contributor to variability in carbonaceous aerosol mass in interior Alaska during the summer by comparing our measurements with satellite data, measurements from an aerosol network and predicted concentrations from a fire inventory coupled to an atmospheric transport model. The $\Delta^{14}C$ of BC from boreal fires was 131 ± 52‰ in the year 2013 when the $\Delta^{14}C$ of atmospheric CO_2 was 23 ± 3‰, corresponding to a mean fuel age of 20 years. Fire-emitted OC had a similar $\Delta^{14}C$ (99 ± 21‰) as BC, but during background (low fire) periods OC (45 to 51‰) was more positive than BC (−354 to −57‰). We also analyzed the carbon and nitrogen elemental and stable isotopic composition of the $PM_{2.5}$. Fire-emitted aerosol had an elevated carbon to nitrogen (C/N) ratio (29 ± 2) and $\delta^{15}N$ (16 ± 4‰). Aerosol $\Delta^{14}C$ and $\delta^{13}C$ measurements were consistent with a mean depth of burning in organic soil horizons of 20 cm (and a range of 8 to 47 cm). Our measurements of fire-emitted BC and $PM_{2.5}$ composition constrain the end-member of boreal forest fire contributions to aerosol deposition in the Arctic and may ultimately reduce uncertainties related to the impact of a changing boreal fire regime on the climate system.

1. Introduction

Black carbon (BC) aerosol is a major climate forcing agent [*Hansen et al*., 2000; *Jacobson*, 2001; *Ramanathan and Carmichael*, 2008]. A recent assessment suggests that BC is the second most important climate warming agent in the present atmosphere after CO_2, with a total radiative forcing of about 1.1 W m^{-2} [*Bond et al*., 2013]. BC originates from incomplete combustion of biomass and fossil fuels and contributes directly to atmospheric warming by absorbing and scattering solar radiation [*Penner*, 1995; *Liousse et al*., 1996; *Myhre et al*., 2013]. Combined with organic carbon (OC) and other aerosol types, BC also influences climate by means of semidirect and indirect effects on clouds [*Ackerman et al*., 2000; *Lohmann and Feichter*, 2005; *Cozic et al*., 2007; *Spracklen et al*., 2008; *Bauer et al*., 2010; *Koch and Del Genio*, 2010; *Ghan et al*., 2012; *Ward et al*., 2012; *Tosca et al*., 2014].

Within the Arctic, warming from BC aerosols is amplified by deposition on snow and ice surfaces, which reduces surface albedo, increases surface solar heating, and accelerates snow and ice melt [*Wiscombe and Warren*, 1980; *Flanner et al*., 2007, 2009; *Hadley and Kirchstetter*, 2012; *Lee et al*., 2013; *Jiao et al*., 2014]. Several modeling studies have attempted to quantify the radiative forcing of BC on snow and ice [*Flanner et al*., 2007, 2009; *Koch et al*., 2009; *Skeie et al*., 2011; *Wang et al*., 2011]. In a metaanalysis, *Bond et al*. [2013] estimated that the BC snow and ice albedo forcing for the industrial era (1750–2005) is 0.13 W m^{-2} with a 90% uncertainty range of 0.04 to 0.33. Because of strong local albedo feedbacks from melting, the efficacy of the BC snow and ice albedo forcing (i.e., the associated change in equilibrium global mean temperature

per unit of radiative forcing compared to equivalent ratio for atmospheric CO_2) is estimated to be 2–4 [*Hansen and Nazarenko*, 2004; *Flanner et al*., 2007]. Thus, mitigating BC emissions may be important in slowing the observed rapid rate of Arctic warming [*Quinn et al*., 2008; *Penner et al*., 2010]. Two important questions remain with respect to the design of effective mitigation policy for BC: (1) What is the relative contribution of fire and fossil sources to BC deposition in different parts of the Arctic? and (2) How will climate change modify these sources, thus contributing to positive or negative feedbacks?

Measurements of BC in arctic snow indicate that boreal forest fire emissions can be an important component of the deposition flux, based on the signature of covarying tracers and optical properties [*Hegg et al*., 2009, 2010; *Doherty et al*., 2010]. Chemical signatures of boreal forest fire emissions have been preserved in Greenland ice records [*McConnell et al*., 2007], and there is some evidence that widespread surface melt events cooccur with deposition of BC from fires [*Keegan et al*., 2014]. Boreal fires can release a large amount of radiative energy [*Levine and Cofer*, 2000; *Val Martin et al*., 2010], leading to the development of convective smoke columns that often extend above the planetary boundary layer [*Fromm*, 2005; *Damoah et al*., 2006; *Kahn et al*., 2008; *Val Martin et al*., 2010]. The injection of plumes into the free troposphere increases the likelihood of long-range transport [*Forster et al*., 2001; *Turquety et al*., 2007; *Chen et al*., 2009]. Modeling studies by *Stohl et al*. [2006, 2013] indicate that during the summer, boreal forest fires are the dominant source of BC in the Arctic. Although atmospheric BC concentrations are much lower in summer compared to late winter and early spring [*Sharma*, 2004], deposition on snow and ice during summer months has a disproportionate influence on the surface radiation budget because of higher levels of downwelling shortwave radiation and the prevalence of strongly reflective low-level stratus cloud decks [*Stohl et al*., 2006; *Flanner et al*., 2007]. *Flanner et al*. [2007] estimated that in a high boreal burning year (1998) about 35% of the total high-latitude BC forcing was due to boreal fires.

While it is clear that boreal forest fires can significantly contribute to the BC transported into the Arctic, current estimates of boreal fire BC emissions remain uncertain and poorly constrained by measurements. Bottom-up model estimates of carbon emissions are uncertain because of challenges in modeling fuel loads and depth of burn (and thus fuel consumption) in organic soil layers of boreal forests [*French*, 2004; *Soja*, 2004; *Turetsky et al*., 2010; *Rogers et al*., 2014; *Veraverbeke et al*., 2015]. Emission factors of BC production per unit of combusted biomass are known to vary as a function of fuel type, fuel moisture content, and flaming versus smoldering combustion phases, further increasing the range of possible estimates [*Reid et al*., 2005; *Koch et al*., 2009; *Akagi et al*., 2011; *French et al*., 2011; *Bond et al*., 2013; *Yokelson et al*., 2013; *Kukavskaya et al*., 2013; *Davis et al*., 2015]. Within the atmosphere, additional uncertainties are introduced from difficulties in simulating BC aging, atmospheric transport, and rates of dry and wet deposition [*Croft et al*., 2005; *Koch et al*., 2009; *Xian et al*., 2009; *Vignati et al*., 2010; *Bond et al*., 2013].

Future changes in the boreal fire regime have the potential to contribute to climate feedbacks [*Randerson et al*., 2006; *Bonan*, 2008; *Bowman et al*., 2009; *Rogers et al*., 2015] by affecting BC emissions and deposition on snow, glaciers, sea ice, and ice sheets [*Hansen and Nazarenko*, 2004; *Flanner et al*., 2007; *Ramanathan and Carmichael*, 2008; *Stone et al*., 2008; *Ward et al*., 2012; *Marks and King*, 2013] and by influencing atmospheric chemistry [*Levine and Cofer*, 2000; *Spracklen et al*., 2008; *Palmer et al*., 2013] and surface biophysics [*Liu*, 2005; *Amiro et al*., 2006; *McGuire et al*., 2006; *Liu and Randerson*, 2008; *Jin et al*., 2012; *Oris et al*., 2014]. Fire frequency and intensity are projected to increase during the remainder of the 21st century as a consequence of longer fire seasons and larger vapor pressure deficits in the middle of the growing season [*Amiro et al*., 2009; *Balshi et al*., 2009; *Euskirchen et al*., 2009; *de Groot et al*., 2013; *Flannigan et al*., 2013; *Boulanger et al*., 2014]. The net effect of these changes on regional and global climate remains uncertain and requires the development of new approaches for quantifying the strength of the various feedback pathways.

Isotopic constraints on fire and fossil fuel contributions have the potential to reduce uncertainties in the partitioning of the total aerosol load, and thereby forcing, measured at remote locations, either in the atmosphere [e.g., *Wang et al*., 2011] or in snow [e.g., *Hegg et al*., 2009, 2010]. The use of radiocarbon (^{14}C) measurements is a particularly effective approach because of the large contrast between fossil fuel (which is ^{14}C free) and biomass burning emissions (which has a $^{14}C/^{12}C$ ratio proportional to atmospheric CO_2 at the time of carbon fixation) [*Reddy et al*., 2002]. Although it has been shown that ^{14}C can successfully be used to partition BC sources (see Table 1 for a summary of studies), the $^{14}C/^{12}C$ end-member for biomass burning is not often

Global Biogeochemical Cycles

10.1002/2015GB005247

Table 1. Biomass Burning (BB) End-Members Used in ^{14}C Source Apportionment Studies[a]

Reference	Location	Compound	Year of Sampling	BB End-Member in $\Delta^{14}C$ (‰)	Turnover Time (± Meas. Error) (years)	Turnover Time Range (years)	Comments
			Direct Measurement				
Klinedinst and Currie [1999]	Colorado, USA	TOC	1999	92.5 ± 12.5[b]	1 (1 to 3)	-	Direct measurements of hardwood
			1999	224 ± 12[b]	19–21 (16 to 28)	-	Direct measurements of softwood
This study	Alaska, USA	BC	2013	131 ± 52	20 (11 to 47)		Direct measurement of boreal fire aerosol using Keeling Plot and background removal approaches
		TC		103 ± 23	14 (11 to 18)		
		OC		99 ± 21	13 (10 to 17)		
			Estimated Using Contemporary Atmospheric $\Delta^{14}CO_2$				
Slater et al. [2002]	Summit, Greenland	BC in snow	1994/1995	114 ± 10[b]	1 (1 up to 2)		Snow samples
Bench [2004]	Yosemite NP, USA	TOC	2002	93 [73–113][b]	4	1 to 6	Average for contemporary samples between 1997–2002
Bench et al. [2007]	9 IMPROVE sites in USA	TOC	2004–2006	73 [43–103][b]	3	1 to 7	Average for contemporary samples between 1999-2003
			Modeled From Tree Growth Rates and Ages				
Szidat et al. [2006]	Zurich, Switzerland	OC and BC	2002/2003	232 [182–282][b]	45–54	16 to 100	Modeled age of residential wood burning of 30–50 year old softwood and hardwood [*Lewis et al.*, 2004]
Gelencsér et al. [2007]	Five rural/remote sites in Europe	TOC, OC and BC	2002–2004	142 [63–242]	12	1 to 100	Model-based average between agricultural residue and maximum tree signature [*Lewis et al.*, 2004]
			Prescribed Using Literature Reports (*Including Above Reports*)				
Zencak et al. [2007]	Methods description	TOC, BC	2005	90–225	-	10 to 61	Range between contemporary $\Delta^{14}CO_2$ and $\Delta^{14}C$ of wood logged in the 1990
Sheesley et al. [2009]	Sweden	TOC	2006	218	48–56	-	-
Gustafsson et al. [2009]	South Asia	BC	2006	199	29–32	-	India-tailored $\Delta^{14}C$ biomass end-member, based on weighted fuel consumption contributions
Yttri et al. [2011]	Nordic Rural Background Sites	OC and BC	2009	47–241[b]	-	1–100	Based on *Szidat et al.* [2009] and contemporary $\Delta^{14}CO_2$ measurements
Heal et al. [2011]	Birmingham, UK	OC and BC	2007–2009	72 [43–142][b]	5	1–15	Based on *Szidat et al.* [2009] and contemporary $\Delta^{14}CO_2$ measurements
Bernardoni et al. [2013]	Northern Italy	OC and BC	2009–2011	75[b]	7	-	Same as [*Minguillón et al.*, 2011]
Chen et al. [2013]	China	BC	2009/10	112	13	-	China-tailored $\Delta^{14}C$ biomass end-member, based on weighted fuel consumption contributions

[a]A hyphen (-) was used to indicate that values were not reported.
[b]Indicates that radiocarbon was reported in Fraction Modern and then converted to $\Delta^{14}C$ (‰), using the year of sampling.

directly measured and may not correspond to the value of contemporary atmospheric CO_2 [*Gustafsson et al*., 2009]. Aboveground thermonuclear weapons testing produced large quantities of ^{14}C in the 1950s and early 1960s causing a sudden twofold increase in the ^{14}C content of the Northern Hemisphere atmosphere [*Telegadas*, 1971; *Nydal and Lövseth*, 1983]. Since the test cessation of aboveground weapons in 1963, the $^{14}C/^{12}C$ ratio of CO_2 has gradually declined as a consequence of exchange with ocean and land reservoirs and dilution by fossil fuel emissions [*Suess*, 1955; *Levin et al*., 2010]. The changing $^{14}C/^{12}C$ ratio of the atmosphere has led to a nonuniform and time-evolving labeling of terrestrial ecosystems as a consequence of carbon flow from the atmosphere through photosynthesis into plant, litter, and soil organic matter pools that have widely varying turnover times [*Trumbore*, 2000].

The heterogeneity of carbon ages within ecosystems makes it challenging to estimate the $^{14}C/^{12}C$ ratio of fire-emitted aerosols. In boreal forests, further complications arise because organic soils have highly variable $^{14}C/^{12}C$ and are known to comprise the vast majority of carbon consumed by fire [*Dyrness and Norum*, 1983; *Kasischke et al*., 1995; *Rogers et al*., 2014]. The $^{14}C/^{12}C$ ratio of organic soils increases with depth because carbon farther from the surface is often older and thus was fixed at a time when the $^{14}C/^{12}C$ of atmospheric CO_2 was higher [*Trumbore and Harden*, 1997; *Carrasco et al*., 2006; *Schuur and Trumbore*, 2006]. This pattern often reverses in deeper soil horizons where the carbon content originates from plant fixation prior to the bomb era and also from the cumulative effects of radioactive decay. As a consequence of these vertical gradients, the $^{14}C/^{12}C$ ratio of emissions is expected to be a nonlinear function of fire severity.

Here we present results from direct measurement of BC and total carbon aerosol from wildfires in interior Alaska during the summer of 2013, collected as a part of NASA's Carbon in Arctic Reservoirs Vulnerability Experiment (CARVE). We isolated BC from fine particulate matter ($PM_{2.5}$) using the Swiss_4S protocol [*Zhang et al*., 2012]. Improvements in the protocol described by *Mouteva et al*. [2015] allowed us to accurately quantify the $^{14}C/^{12}C$ ratio of the aerosol samples, along with uncertainties introduced from sample processing. We show that fires were the dominant contributor to variability and aerosol mass in interior Alaska during the summer of 2013 by combining our measurements with satellite observations and atmospheric models. We find that the $^{14}C/^{12}C$ of BC aerosol during periods dominated by fire emissions was considerably higher than measurements from atmospheric CO_2 at Point Barrow. Taking advantage of the synoptic-scale temporal variability, we use a Keeling Plot approach to estimate the isotopic composition of the fire aerosol end-member. Additional aerosol and soil organic matter elemental and isotopic measurements indicate that aerosols provide information about the depth of burning in organic soils and that combustion and atmospheric processing enrich the $\delta^{15}N$ of fine particulate matter.

2. Methods

2.1. Study Sites

We collected aerosol samples at two locations in interior Alaska during the summer of 2013 (27 June to 10 August). One site was located at Caribou Poker Creek Long-Term Ecological Research Station (hereafter referred to as "Caribou"; 65.13°N, 147.45°W) and the other at Delta Junction Agricultural and Forestry Experimental Site (hereafter "Delta"; 63.97°N, 145.40°W). These two locations, separated by 168 km, were selected to enable sampling of fire-emitted aerosols in different areas of interior Alaska (Figure 1a).

To help relate carbonaceous aerosol measurements to soil emissions, we also analyzed a set of four soil profiles collected in August of 2012 in unburned (control) areas near the Gilles Creek fire perimeter (C02: 64.33°N, 145.88°W; C04: 64.31°N, 145.94°W; C05: 64.32°N, 145.89°W; C06: 64.36°N, 145.58°W), described by *Rogers et al*. [2014]. The Gilles Creek fire burned during May of 2010 and covered 78.4 km^2. We chose to analyze soil cores from four nearby control sites, representing the ecosystem types burned during the fire. These included the following: (1) lowland black spruce (*Picea mariana* (Mill.) BSP) underlain with permafrost, (2) lowland black spruce without permafrost, (3) upland black spruce, and (4) mixed white spruce (*Picea glauca* (Moench) Voss) and aspen (*Populus tremuloides* Michx.) forests.

2.2. Aerosol Sampling

We used high-volume total suspended particulate samplers (HIVOL-AMCLD, Thermo Environmental Instruments, Franklin, MA, USA) with $PM_{2.5}$ impactor plates (TE-230-QZ, Tisch Environmental, Cleves, OH, USA). The aerosol

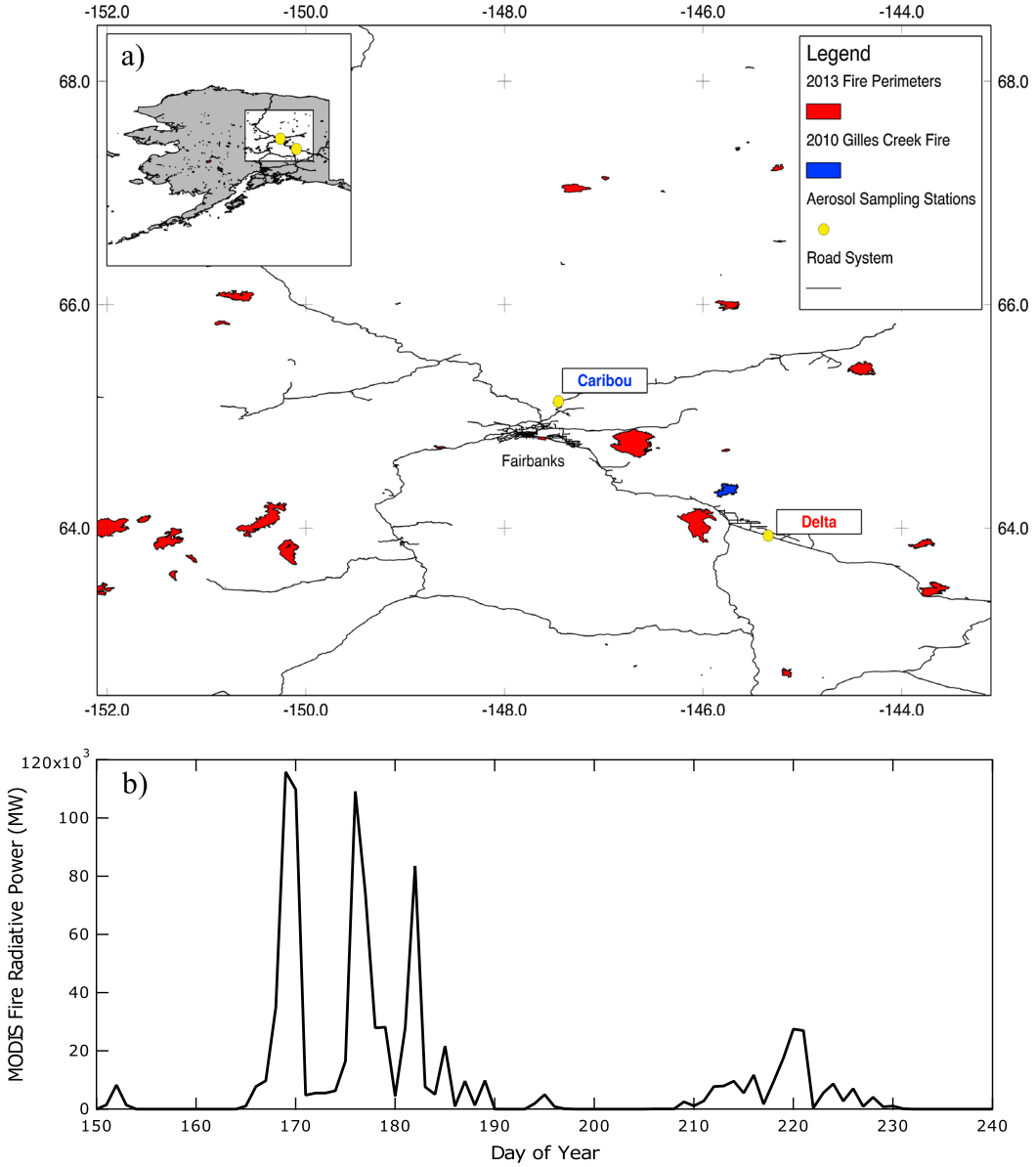

Figure 1. (a) Map of the aerosol sampling stations in interior Alaska and (b) the daily sum of fire radiative power from active fires in interior Alaska, as measured by the Moderate Resolution Imaging Spectrometer on NASA's Aqua and Terra satellites. The 2013 fire perimeters are shown in red and the 2010 Gilles Creek fire is shown in blue. The fire perimeter data were obtained from the Alaska Interagency Coordination Center (AICC). Of the active fires detected by MODIS, 89% were located within the perimeter of fires reported in the AICC Large Fire Database. For the 11% that were not inside these perimeters, most were located in close vicinity (within 1 km) of the perimeter edge.

samplers were operated at a volumetric flow rate of 1300 L min^{-1} to yield a $PM_{2.5}$ sample on a 20 cm × 25 cm quartz microfiber filter (2500 QAT-UP, Pallflex Tissuquartz, Pall, Port Washington, NY, USA). Prior to use, sample filters were prebaked at 500°C for 4 h, wrapped in aluminum foil and stored in sealed plastic bags to prevent contamination. One slotted microquartz fiber filter (TE-230-QZ, microquartz slotted collection substrates, Tisch) was installed in the aerosol sampler impactor head per sampling period to remove particles with an aerodynamic diameter greater than 2.5 μm. The impactor filters were only used for sizing, and were discarded following sampling. A blank filter (1/4 of a prebaked sample filter) was mounted on the inside of each aerosol sampler housing with no gas flow during each sampling period to serve as blank for volatile organic carbon take-up. After collection, sample filters and blanks were wrapped in aluminum foil, packed into airtight plastic bags, and stored at −20°C.

Table 2. Elemental and Radiocarbon Analysis of Carbonaceous Aerosol[a]

Sample Period	Day of year	BC ($\mu g\,m^{-3}$)	BC $\Delta^{14}C$ (‰)	TC ($\mu g\,m^{-3}$)	TC $\Delta^{14}C$ (‰)	OC ($\mu g\,m^{-3}$)[d]	OC $\Delta^{14}C$ (‰)[d]
			Caribou				
27–29 Jun[b]	178–180	0.23	−10 ± 24	7.33	73 ± 3	7.10	76 ± 3
29 Jun to 1Jul[b]	180–182	0.23	13 ± 77	21.03	102 ± 3	20.79	103 ± 3
3–7 Jul[b]	184–188	0.29	58 ± 46	10.20	96 ± 3	9.91	97 ± 3
7–11 Jul[b]	188–192	1.12	106 ± 11	26.63	115 ± 3	25.51	116 ± 3
11–25 Jul[c]	192–206	0.09	−354 ± 60	0.92	13 ± 3	0.83	51 ± 7
25–29 Jul[c]	206–210	0.07	-	1.17	−48 ± 3	1.10	-
29 Jul to 1Aug[c]	210–213	0.06	-	1.28	−23 ± 3	1.22	-
1–8 Aug	213–220	0.11	−136 ± 65	3.20	64 ± 3	3.08	72 ± 4
			Delta				
28–30 Jun[b]	179–181	1.31	94 ± 14	18.82	87 ± 3	17.50	86 ± 3
2–4 Jul[c]	183–185	0.03	-	0.63	-	0.61	-
4–23 Jul[c]	185–204	0.04	−57 ± 65	1.21	42 ± 3	1.17	45 ± 4
23 Jul to 2 Aug[c]	204–214	0.03	-	1.19	28 ± 3	1.16	-
2–7 Aug	214–219	0.07	−14 ± 60	2.91	80 ± 3	2.85	82 ± 3
7–10 Aug[b]	219–222	0.13	32 ± 50	4.17	86 ± 3	4.04	88 ± 3

[a]No value is reported if samples were too small to provide reliable isotopic measurements.
[b]High fire samples.
[c]Background samples.
[d]OC values are calculated as the difference between TC and BC and $\Delta^{14}C$ of OC was calculated using mass balance.

Atmospheric sampling intervals for individual filters ranged from 2 to 19 days (Table 2). The sampling time of aerosol collection varied to allow accumulation of sufficient BC aerosol for ^{14}C analysis and was based on visual inspection of the filter loading. We collected 14 aerosol samples: 8 at Caribou and 6 at Delta.

2.3. Sample Analyses

2.3.1. Isolation of BC From $PM_{2.5}$

To isolate and measure the BC content of each aerosol sample from the organic carbon (OC) fraction, we used a thermo-optical OC/EC analyzer (Sunset Laboratory Inc., Tigard, OR, USA) with the "Swiss_4S" thermal-optical protocol [*Zhang et al*., 2012]. The Swiss_4S protocol enables physical separation of BC from the total carbonaceous aerosol with minimal contamination from nonsample carbon [*Zhang et al*., 2012; *Mouteva et al*., 2015]. A simple and efficient vacuum line was coupled to the OC/EC analyzer, allowing us to cryogenically trap the evolving CO_2 during the thermal-optical analysis for subsequent ^{14}C measurements [*Mouteva et al*., 2015]. Aerosol filter samples were introduced into the OC/EC analyzer as 1.5 cm^2 filter punches (1 cm × 1.5 cm) on a flat quartz spoon. Punches were washed with Milli-Q water (Synergy 185, EMD Millipore, Billerica, MA, USA) prior to analysis to remove water soluble OC and minimize charring.

2.3.2. $\Delta^{14}C$ Analysis of Black Carbon in $PM_{2.5}$

The BC-derived CO_2 was quantified manometrically and sealed into a Pyrex ampoule. On another vacuum line, the CO_2 was converted to graphite using the hydrogen reduction method specifically optimized for ultrasmall samples [*Santos et al*., 2007]. The ^{14}C content of BC was measured via accelerator mass spectrometry (AMS) at the W. M. Keck Carbon Cycle Accelerator Mass Spectrometry laboratory (KCCAMS) of UC Irvine, alongside graphitization standards and blanks. We used the $\Delta^{14}C$ notation (‰) for the presentation of our results (equation (1)):

$$\Delta^{14}C = \left(FM \times e^{\frac{1950-y}{8267}} - 1\right) \times 1000 \quad (1)$$

where y is the year of ^{14}C sampling and FM is the fraction modern, or the $^{14}C/^{12}C$ ratio of the sample divided by the $^{14}C/^{12}C$ ratio of the oxalic acid I standard measured in 1950 ($^{14}C/^{12}C_{ox-I} = 1.176 \pm 0.010 \times 10^{-12}$) corrected for mass-dependent fractionation [*Stuiver and Polach*, 1977], 8267 years is the mean lifetime of ^{14}C, and 1950 is the reference year.

We applied ^{14}C corrections to account for carbon introduced during the analytical procedure using filter blanks and ^{14}C measurements of BC reference materials [*Mouteva et al*., 2015]. For BC samples during high fire periods ($n = 6$), the fraction of extraneous carbon mass added during the analysis procedure (and corrected for) was 15 ± 9%. Note that due to the small sample size of BC aerosol (on the order of a few

micrograms), even small amounts of extraneous carbon can significantly contribute to uncertainties in the $\Delta^{14}C$ measurement [*Mouteva et al.*, 2015]. As a result, uncertainties reported below for the $\Delta^{14}C$ of BC are considerably larger than those for total carbon (TC).

2.3.3. $\Delta^{14}C$ Analysis of Total Carbon in $PM_{2.5}$

Multiple punches ($n = 2$–18, based on carbon content) were taken from each sample and analyzed for the $\Delta^{14}C$ of the total carbon (TC) on the filter. The samples were sealed with CuO under vacuum in precombusted, 9 mm OD quartz tubes and combusted at 900°C for 3 h. Since the filter's TC content was much higher than the BC content, TC samples were graphitized using a modified sealed tube zinc reduction method [*Xu et al.*, 2007]. The $\Delta^{14}C$ of the TC was measured at the KCCAMS facility as described for BC above.

For samples larger than 0.3 mg C, a separate CO_2 aliquot was taken prior to graphitization for $\delta^{13}C$ analysis (see section 2.3.4) with isotope ratio mass spectrometry (IRMS; GasBench II, Deltaplus, Thermo Scientific (Finnigan), Waltham, MA, USA). Filters were not acidified, because the $\delta^{13}C$ of the bulk filters (-27.2 ± 0.2‰) did not indicate the presence of inorganic carbon.

Since the OC fraction of the aerosol is defined as the difference between TC and BC [*Gelencser*, 2004], we were able to derive the ^{14}C content of OC by isotope mass balance (equation (2)):

$$\Delta^{14}C_{OC} = \frac{TC \times \Delta^{14}C_{TC} - BC \times \Delta^{14}C_{BC}}{TC - BC} \tag{2}$$

2.3.4. Elemental and Stable Isotopic Analyses of Bulk $PM_{2.5}$

Aerosol samples were also analyzed for their total carbon and nitrogen (N) content and stable isotope ratios with an elemental analyzer (EA, NA 1500 NC, Thermo Scientific, Waltham, MA, USA) coupled with IRMS (DeltaPlus, Thermo Fisher Scientific (Finnigan), Waltham, MA, USA) at the KCCAMS facility. Total carbon and N concentrations were normalized based on the flow rate of the aerosol samplers and sampling duration to yield concentrations per cubic meter of air. Stable isotope measurements are reported using conventional δ notation (‰) (equation (3)):

$$\delta = \left(\frac{R_{sample}}{R_{standard}} - 1\right) \times 1000 \tag{3}$$

where R_{sample} denotes the heavy-to-light isotope ratio of the aerosol or soil sample and $R_{standard}$ is the isotope ratio of the standard (0.0112372 for Vienna Pee Dee Belemite $^{13}C/^{12}C$ standard [*Gonfiantini*, 1984] and 0.003676 for air $^{15}N/^{14}N$ standard [*Nier*, 1950]. Filter blanks of both TC and N masses, and $\delta^{13}C$ and $\delta^{15}N$ ratios of these blanks were used to remove TC and N introduced during the analytical procedure by isotope mass balance. To get a more representative $\delta^{13}C$ result, we combined the gas bench and the elemental analyzer measurements and calculated weighted averages based on the number of filter punches used for each measurement.

2.3.5. Soil Sample Analyses

Each of the four soil cores was separated into three soil horizons upon collection from top to bottom: moss, fibric, and mesic. Soil samples were dried, weighed, and homogenized with a Wiley mill with a 40 μm sieve. Bulk density and %C content were measured by *Rogers et al.* [2014]. Aliquots of the homogenized soils from each horizon were weighed out and analyzed for their TC and N elemental composition and stable isotopes $\delta^{13}C$ and $\delta^{15}N$ by EA-IRMS. Separate aliquots were weighted out, graphitized via zinc reduction [*Xu et al.*, 2007] and analyzed for their ^{14}C content by AMS. All of the measurements represent a vertical average for each homogenized soil horizon.

2.4. Remote Sensing of Fire Activity

To quantify the daily number of active fire/thermal anomalies in interior Alaska during the study period, we used imagery from the Moderate Resolution Imaging Spectroradiometer (MODIS) on NASA's Aqua and Terra satellites. Our domain was defined to encompass a region spanning 58°–71.5°N and 141°–171°W, with the majority of fires occurring in black spruce forests in the interior. We obtained the global monthly fire location product (MCD14ML) at 1 km resolution from the University of Maryland Active Fire Products website at ftp://fuoco.geog.umd.edu. MCD14ML is a list of the combined Terra and Aqua MODIS Level 2 swath MOD14/MYD14 active fires and includes information about the location of the centroid of each thermal anomaly detection, scan angle, fire radiative power, and a quality flag representing the data confidence level. Since the commission error of the MCD14ML product is low in boreal forest ecosystems, we used all of the

active fire/thermal anomaly observations with low, medium, and high confidence to quantify the temporal dynamics of fire activity.

2.5. Model Predictions of BC Concentrations

Black carbon emissions from fires were modeled by combining the Alaska Fire Emissions Database (AKFED) model [*Veraverbeke et al*., 2015] with the coupled Weather Research and Forecasting-Stochastic Time-Inverted Lagrangian Transport (WRF-STILT) model [*Henderson et al*., 2015]. AKFED is an empirical model of carbon consumption by fire for Alaska with a spatial resolution of 450 m and a temporal resolution of 1 day [*Veraverbeke et al*., 2015]. WRF-STILT is a tool that can be used to calculate backward trajectories of trace gas or particulate fluxes [e.g., *Nehrkorn et al*., 2010]. Carbon emissions from AKFED were converted with an emission factor of 0.5 g BC per 1 kg biomass, based on *Akagi et al*. [2011], and integrated with the WRF-STILT model to estimate BC concentrations from fires at the Caribou and Delta aerosol sampling stations. We used the WRF-STILT simulations coupled with AKFED emissions to provide a qualitative estimate of periods of high and low fire emissions. Estimates of BC from these simulations likely had a high bias because the version of WRF-STILT used here did not include an explicit representation of wet or dry aerosol deposition and assumed that all fire emissions were injected in the lower half of the boundary layer.

2.6. Comparison With Measurements From the Interagency Monitoring of Protected Visual Environments Network

We compared our BC and OC time series with observations from the Interagency Monitoring of Protected Visual Environments (IMPROVE) aerosol network [*Malm and Sisler*, 1994]. We obtained observations from three IMPROVE stations north of the Alaska Range: Trapper Creek (TRCR; 62.3153°N, −150.3156°W, elevation: 155 m above sea level; asl), Denali National Park (DENA; 63.7233°N, −148.9675°W, 658 m asl), and Gates of the Arctic (GAAR; 66.9025°N, −151.5170°W, 196 m asl). Each measurement in the IMPROVE time series represents an average over a 24 h period, and samples are collected every 3 days. BC and OC are measured using the IMPROVE_A thermal protocol, described by *Chow et al*. [2007] These data were obtained from the IMPROVE website (http://vista.cira.colostate.edu/improve/) in February, 2015.

3. Results

3.1. Fire Activity and Carbonaceous Aerosol Concentrations

The 2013 fire season in interior Alaska was characterized by two periods of high fire activity, as described using the daily sum of fire radiative power measured by MODIS sensors on Terra and Aqua satellites (Figure 1b). The first high fire period occurred during 17 June to 8 July (day of year 168 to 189) and overlapped with the beginning of our aerosol measurement campaign. A second period occurred during 1–14 August (day of year 213 through 226) and overlapped with our final set of sampling intervals. A middle period with little or no daily fire activity from 8 July to 1 August (day of year 190 through 212) was characterized by several precipitation events and lower vapor pressure deficits.

At both stations, the concentrations of BC and OC covaried with the timing of fire activity (Figures 2a–2d and Table 2). The highest detected BC concentrations were 1.12 $\mu g/m^3$ for Caribou during 7–11 July and 1.31 $\mu g/m^3$ for Delta during 28–30 June, with both maxima overlapping with the first high fire period. Elevated BC concentrations were also detected during the second high fire period, with 0.11 $\mu g/m^3$ measured at Caribou during 1–8 August and 0.13 $\mu g/m^3$ at Delta during 7–10 August. Compared with the relatively low BC concentrations measured during middle to late July (denoted as background samples in Table 2), the first high fire period was associated with an order of magnitude increase in BC, while the second high fire period had a 50% to 290% increase.

The OC and TC concentrations followed a similar temporal pattern as BC (Figures 2c and 2d and Table 2), indicating that all of the components of carbonaceous aerosol load were responding to the same set of aerosol emission and atmospheric transport processes. The highest OC concentrations were 25.5 $\mu g/m^3$ for Caribou and 17.5 $\mu g/m^3$ at Delta and were measured during the same periods when BC concentrations were highest (Figures 2c and 2d).

Three types of supporting information provided evidence that fires were the dominant contributor to the aerosol variability observed at these stations and that impact of fires on aerosols was widespread in Alaska

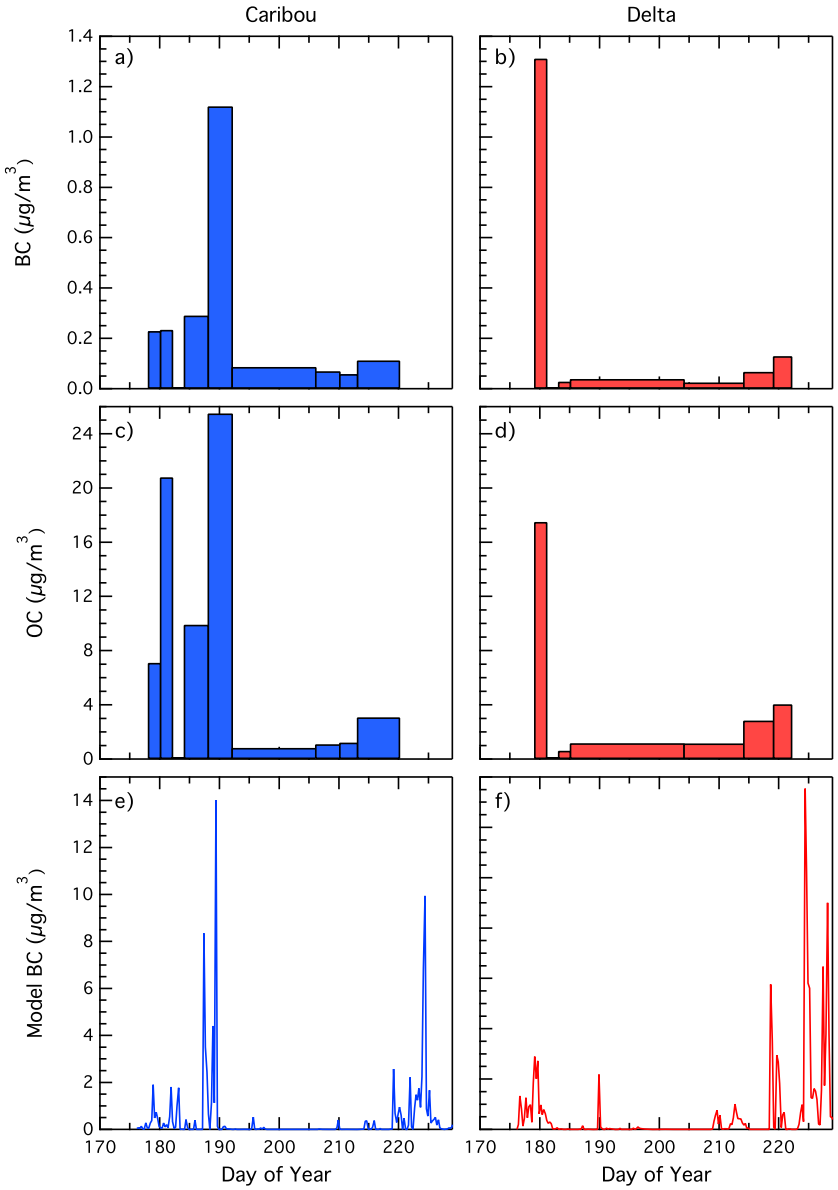

Figure 2. Measured aerosol concentrations of (a and b) black carbon (BC) and (c and d) organic carbon (OC) compared to (e and f) model BC predictions. The results are shown for the Caribou station in blue and Delta station in red. Observations are normalized for the sampling time and flow rate. Model predictions are derived from the daily AKFED fire inventory combined with WRF-STILT and plotted at a 6 h time step. The higher temporal resolution of the model estimates in Figures 2e and 2f yielded larger concentrations than the observations during short intervals with intense fire influence.

during the 2013 summer. First, modeled BC concentrations from the fire emissions inventory (AKFED) coupled to the regional atmospheric model (WRF–STILT) predicted elevated BC concentrations from fires near the beginning and end of our sampling period, similar to the observed pattern (Figures 2e and 2f). Since only fires from Alaska are included in AKFED, these model simulations confirmed that boreal forest fires were the primary driver of the aerosol variability measured at these locations. Second, comparison with data from IMPROVE indicated that the BC and OC measurements at Caribou and Delta had similar magnitude and temporal variability as the aerosols sampled at nearby IMPROVE stations (Figure 3). Two of the northernmost stations—Denali National Park and Gates of the Arctic—had elevated BC and OC concentrations during late June and early July and during the first two weeks of August, corresponding to the two high fire periods observed during our sampling campaign. While our measurements of OC from Caribou and Delta were higher than IMPROVE measurements at Denali and Gates of the Arctic during early July, this difference is

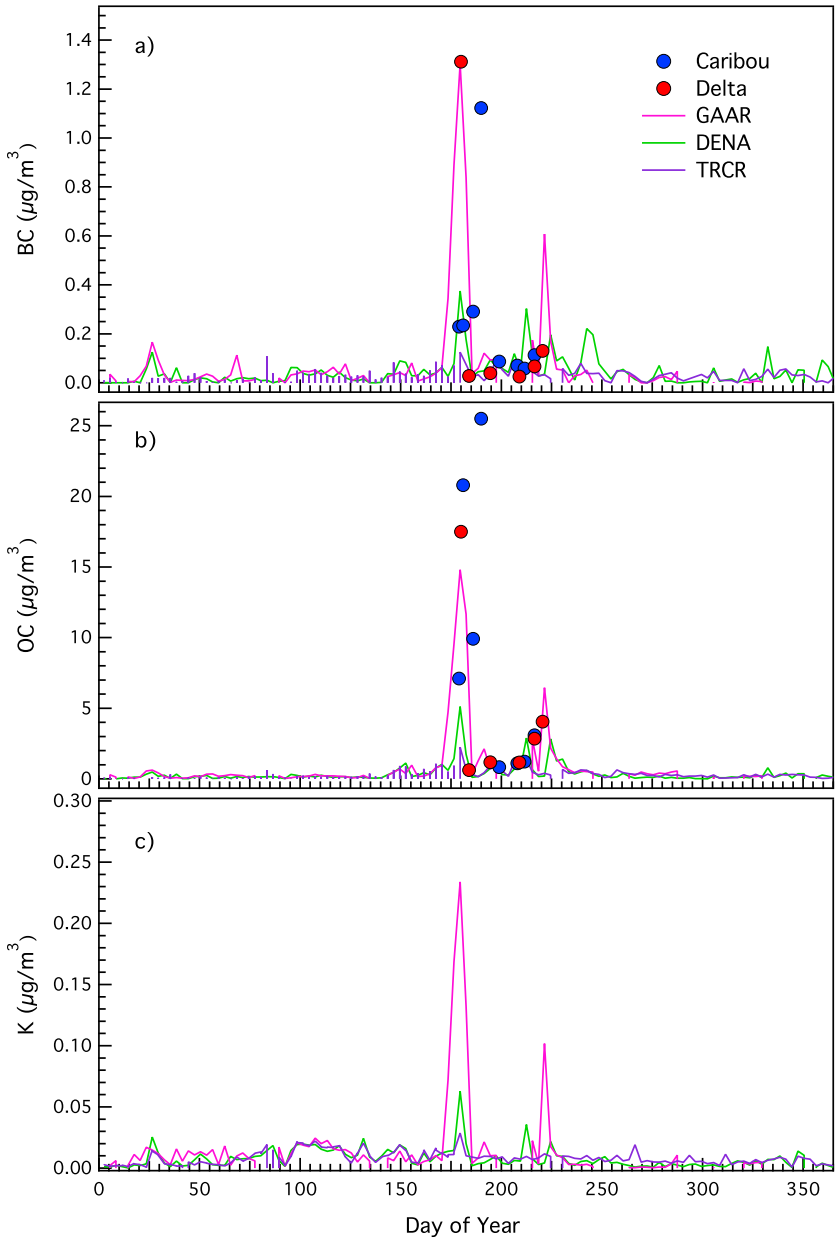

Figure 3. Comparison of (a) BC and (b) OC concentrations measured in this study with time series from the IMPROVE stations Gates of the Arctic National Park (GAAR), Denali National Park (DENA), and Trapper Creek (TRCR) in Alaska for the year 2013. (c) The IMPROVE measurements of potassium (K), a well-known biomass burning tracer.

consistent with the closer proximity of the Caribou and Delta sampling stations to the perimeter of large wildland fires that burned in interior Alaska during the summer of 2013. Potassium (K) measurements from IMPROVE were elevated at the Gates of the Arctic and Denali National Park stations during these periods, which is consistent with the aerosols having a fire origin [e.g., *Andreae et al.*, 1984]. Third, our aerosol $\Delta^{14}C$ analysis, described in the following section, further confirmed that fires were the dominant contributor to the aerosol variability, since the times of highest carbonaceous aerosol concentration were also the times when $\Delta^{14}C$ was most positive, indicating a strong biogenic source and a negligible fossil contribution.

3.2. Aerosol $\Delta^{14}C$ Variability

The $\Delta^{14}C$ of BC, TC, and the calculated OC positively covaried with concentration and was considerably more positive during the two high fire periods (Figure 4, Table 2). For BC, the highest measured $\Delta^{14}C$

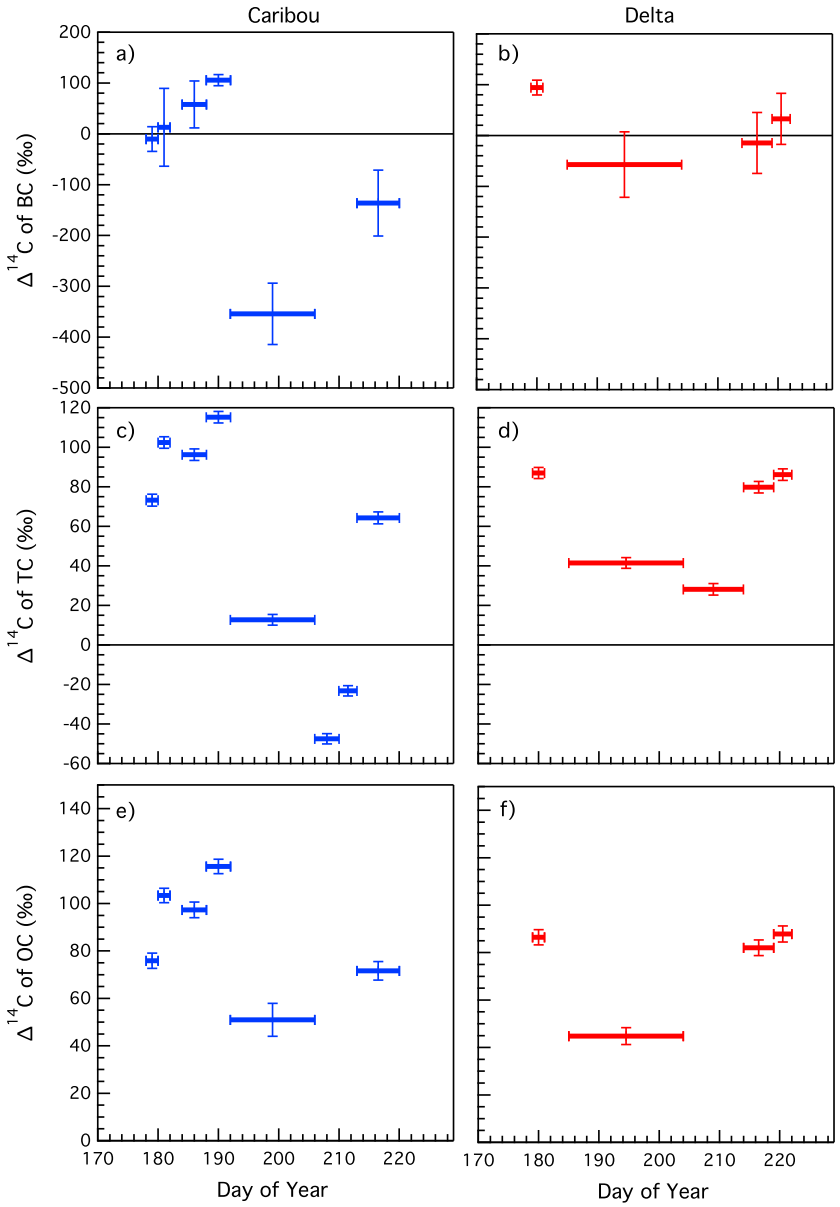

Figure 4. Radiocarbon measurements of (a and b) BC and (c and d) TC and (e and f) OC at Caribou (blue) and Delta (red) stations. The BC concentration on some of the samples were too low for radiocarbon analysis; hence, there are more data points for TC than for BC. Data were corrected for procedural contaminations and the corresponding uncertainty is shown.

was 106 ± 11‰ at Caribou and 94 ± 14‰ at Delta, while in the year 2013 the $\Delta^{14}C$ of atmospheric CO_2 at Point Barrow was 23 ± 3‰ (X. Xu, unpublished data, 2015). In comparison, minimum values of −354 ± 60‰ at Caribou and −57 ± 65‰ at Delta occurred during intervals with low fire activity (Figures 4a and 4b). For several sampling periods, BC concentration was too small for ^{14}C analysis (Table 2).

The $\Delta^{14}C$ of TC had a similar temporal pattern as BC, with more positive values corresponding to high fire periods. The highest measured $\Delta^{14}C$ of TC was for samples that had the highest aerosol concentration: 115 ± 3‰ for Caribou and 87 ± 3‰ for Delta. Overall, TC had more positive values of $\Delta^{14}C$ than BC, and the difference between the $\Delta^{14}C$ of TC and BC was largest during low fire periods, indicating that the ^{14}C content of background BC was more depleted than TC. The lowest measured $\Delta^{14}C$ of TC was −48 ± 3‰ at Caribou and 28 ± 3‰ at Delta; these samples had BC concentrations too low for ^{14}C analysis (Figures 4c and 4d).

Table 3. Fire-Derived $\Delta^{14}C$ (‰) Signature of Black Carbon (BC), Total Carbon (TC), and Organic Carbon (OC)

	Background			Background			Background[a]		
Method Used	BC ($\mu g\ m^{-3}$)	BC $\Delta^{14}C$ (‰)	Fire-Emitted BC $\Delta^{14}C$ (‰)	TC ($\mu g\ m^{-3}$)	TC $\Delta^{14}C$ (‰)	Fire-Emitted TC $\Delta^{14}C$ (‰)	OC ($\mu g\ m^{-3}$)	OC $\Delta^{14}C$ (‰)	Fire-Emitted[a] OC $\Delta^{14}C$ (‰)
				Caribou					
Keeling Plot[b]	-	-	186 ± 34 ($r^2 = 0.94$)	-	-	110 ± 16 ($r^2 = 0.80$)	-	-	102 ± 8 ($r^2 = 0.69$)
Background removal.	0.07	−354	168 ± 28	1.12	−19.33	107 ± 13	1.05	51	102 ± 16
				Delta					
Keeling Plot[b]	-	-	89 ± 12 ($r^2 = 0.97$)	-	-	100 ± 7 ($r^2 = 0.93$)	-	-	98 ± 6 ($r^2 = 0.91$)
Background removal	0.03	−57	81 ± 25	1.01	35	96 ± 9	0.98	45	95 ± 9
Average			131 ± 52			103 ± 23			99 ± 21

[a]OC was calculated as the difference between TC and BC, and $\Delta^{14}C$ was derived via mass balance.
[b]For all Keeling plots regression analyses, r^2 values are provided in parenthesis next to the intercept value.

Since BC was only a small fraction of TC mass, the calculated $\Delta^{14}C$ of OC (see section 2.3.3.) was very close to that of TC during periods of high fire activity. The highest estimated $\Delta^{14}C$ of OC was 116 ± 3‰ at Caribou and 88 ± 3‰ at Delta, nearly equivalent to the $\Delta^{14}C$ of TC reported for these samples. The $\Delta^{14}C$ of OC background samples was estimated only where $\Delta^{14}C$ of BC and TC were simultaneously measured. With this constraint, the $\Delta^{14}C$ of the OC background was higher than TC or BC, with values of 51 ± 7‰ at Caribou and 45 ± 4‰ at Delta (Figures 4e and 4f). These site level differences in the background aerosol $\Delta^{14}C$ may reflect a different proximity of the two stations to regional urban sources, with the Caribou station located about 35 km to the northeast of the city of Fairbanks and Delta about 153 km to the southeast (Figure 1a).

3.3. Isolating the $\Delta^{14}C$ of Fire-Emitted BC, TC, and OC

To quantify the $\Delta^{14}C$ signature of fire-emitted aerosol, we used two approaches (Table 3). The first approach was to construct a Keeling Plot using concentration and $\Delta^{14}C$ measurements for each aerosol component (Figure 5). Keeling Plots have been widely used for identification of the isotopic composition of trace gases [*Pataki*, 2003] and to assess sources of dissolved organic carbon in marine ecosystems [*Mortazavi and Chanton*, 2004]. The second approach was to remove a mean background concentration and isotope ratio from the high fire samples. The background was estimated independently for each station from samples collected during periods of low fire activity. High fire and low fire samples are denoted with footnotes in Table 2.

The Keeling Plot showed that $\Delta^{14}C$ and the inverse of concentration of BC at each site were highly correlated, with R^2 values greater than 0.94 (Figure 5a and Table 3). The robustness of the type II regression coefficients provided confidence that the technique successfully identified the fire end-member. Using this approach, the $\Delta^{14}C$ of fire-emitted BC was estimated to be 186 ± 34‰ at Caribou and 89 ± 12‰ at Delta, where the reported error is the intercept uncertainty of the Keeling Plot. The $\Delta^{14}C$ of fire-emitted TC was consistent within the uncertainty between the two stations and was lower than the BC estimate at Caribou (110 ± 16‰) and higher at Delta (100 ± 7‰) (Figure 5b). The $\Delta^{14}C$ of fire-emitted OC, derived from estimated concentration and $\Delta^{14}C$, was much closer between the two stations: 102 ± 8‰ at Caribou and 98 ± 6‰ at Delta (Figure 5c).

The second approach for determining the fire $\Delta^{14}C$ end-member was to estimate a background aerosol concentration and $\Delta^{14}C$ and then to subtract it from all of the high fire samples at each station. High fire samples were identified as having concentrations of BC greater than 0.11 $\mu g/m^3$ and TC greater than 3.20 $\mu g/m^3$. In parallel, the background was determined separately at each station, consisting at Caribou as the mean of all samples with BC $\leq$ 0.09 $\mu g/m^3$ and TC $\leq$ 1.28 $\mu g/m^3$ and at Delta as the mean of samples with BC $\leq$ 0.04 $\mu g/m^3$ and TC $\leq$ 1.21 $\mu g/m^3$. Note that several sampling intervals had intermediate concentrations and thus were excluded from this analysis.

Using the background subtraction approach, we estimated that the $\Delta^{14}C$ of fire-derived BC (mean $\pm$ 1 standard deviation (σ)) was 168 ± 28‰ ($n = 4$ high fire samples) at Caribou and 81 ± 25‰ ($n = 2$ high fire samples) at Delta. Similarly, TC estimates were 107 ± 13‰ and 96 ± 9‰ at the two stations, and OC estimates were 102 ± 16‰ and 95 ± 9‰.

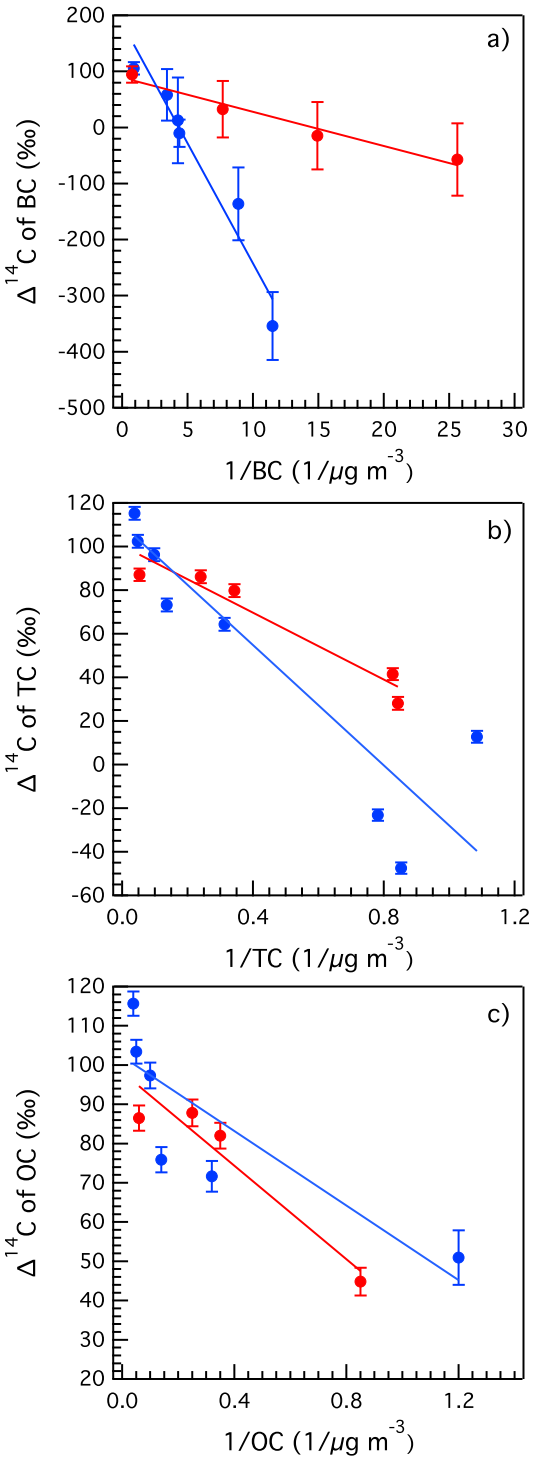

Figure 5. Keeling plot analysis for (a) BC and (b) TC and (c) OC for the Caribou (blue) and Delta (red) stations, respectively. The linear regressions are calculated separately for each station and the results are summarized in Table 3.

Averaging across the two sites and the two approaches used to estimate the fire end-member (i.e., the Keeling Plot and background removal approach), the Δ^{14}C of fire-emitted BC was 131 ± 52‰ (mean ± 1σ, Table 3). Using the same methodology, the Δ^{14}C of fire-emitted TC was 103 ± 23‰ and the Δ^{14}C of fire-emitted OC was 99 ± 21‰. The uncertainty associated with these regionwide estimates originated from several sources, including (1) the sampling of different fires at the two stations, (2) temporal variations in the depth of burn into soil organic matter layers in response to variations in fire weather and other environmental controls, and (3) methodological differences in the two approaches used for isolating the fire end-member. With respect to the third error source, the Keeling Plot and background subtraction relied on different aspects of the observed time series. The two approaches, however, yielded similar estimates at each station (had overlapping uncertainty ranges), providing confidence in the final estimate.

3.4. The Mean Age of Fire-Emitted Aerosol

The Δ^{14}C of the fire end-member provided a partial constraint on the age of fuels consumed by the fires during 2013. Assuming the BC originated from surface soil organic matter layers and aboveground biomass that could be represented with a single mean turnover time, and using a time series of $\Delta^{14}CO_2$ derived from measurements at Point Barrow and other Northern Hemisphere stations, we estimated that the combusted fuels contributing to Δ^{14}C of BC had mean age of 20 years (Figure 6). The ±1σ of BC Δ^{14}C of ± 52‰ yielded an asymmetric age range of 11 to 47 years when convolved with the atmospheric record. Similarly, we estimated fuel ages of 14 years (with a range of 11 to 18 years) for TC and 13 years (with a range of 10 to 17 years) for OC.

3.5. Aerosol Elemental and Stable Isotope Composition

The C/N ratio of the $PM_{2.5}$ was elevated during high fire periods at both stations (Figures 7a and 7b and Table 4). At Caribou, we measured C/N ratio of 24 ± 1 (mean ± 1σ, $n = 4$) during high fire periods, and 10 ± 3 ($n = 3$) in background air. Similarly, the average C/N ratio at Delta was 33 ± 8 ($n = 2$) during high fire periods, and 17 ± 9 ($n = 3$) for the background. To estimate and subtract the background contribution to the C/N ratio, we used the average of our TC and N measurements from the background samples and subtracted them from the high fire samples at each station (Table 4). This yielded high fire C/N ratios of 29 ± 2 at Caribou and 63 ± 47 at Delta. The high range observed at Delta was driven by one sample (7–10 August)

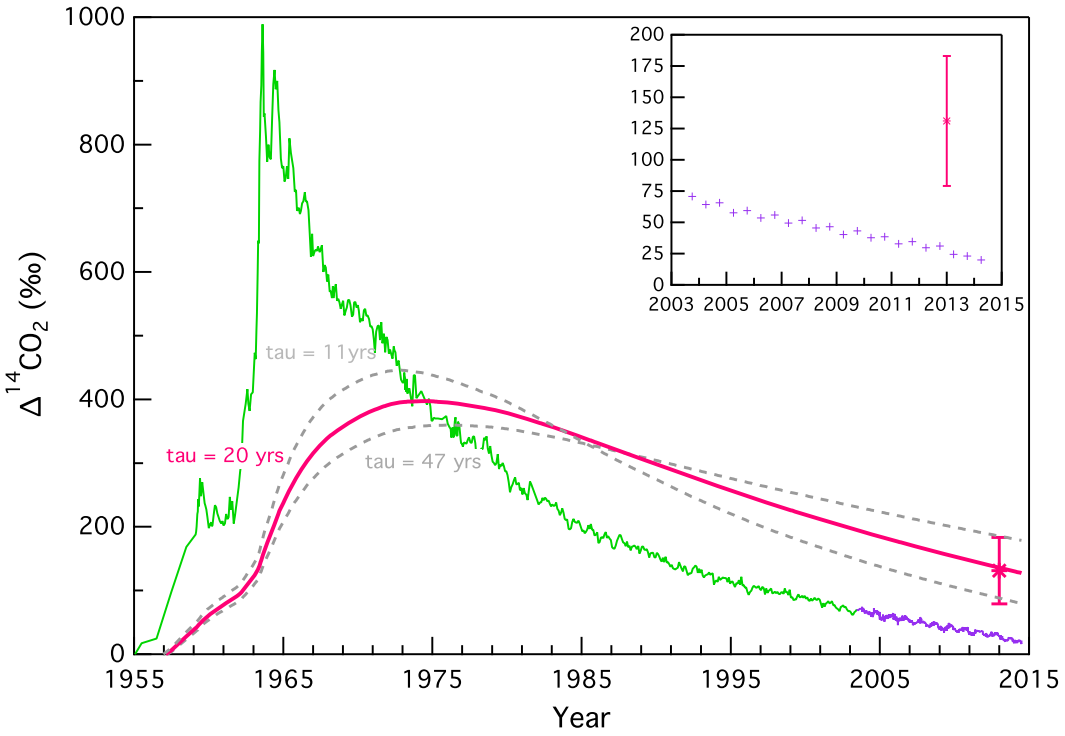

Figure 6. The time evolving $\Delta^{14}C$ of boreal fire-emitted BC and atmospheric $\Delta^{14}CO_2$ from 1955 to 2015. The BC aerosol trajectory was estimated using the observations from 2013 and assuming the fire emissions originated from a carbon pool with a single, constant turnover time. Atmospheric $\Delta^{14}CO_2$ data from 1950 from the Heidelberg sampling network was obtained from *Levin et al.* [2010] (green) and combined with observations from Point Barrow from 2004 to 2015 (X. Xu, unpublished data, 2015; purple line). The top right inset focuses on the period since 2004.

with N concentration almost the same as the background. Averaging across all high fire samples at both stations, we obtained a mean fire-derived C/N ratio of 40 ± 28 ($n = 6$). Excluding the one sampling interval from Delta with the lowest TC and N almost equivalent to background, the fire C/N ratio decreased to 29 ± 2 ($n = 5$).

The $\delta^{15}N$ of aerosol sampled during high fire periods also was considerably higher than levels collected during background periods (Figures 7c and 7d and Table 4). At Caribou high fire samples had a mean $\delta^{15}N$ value of 12.2 ± 1.1‰ ($n = 4$) that was similar to the single value of 12.7‰ measured at Delta. During the low fire background period Caribou had a negative $\delta^{15}N$ of −4.3‰ ($n = 1$) and Delta had a mean of 1.9‰ ($n = 2$). Note that the N content of many samples was too low to allow reliable isotopic analysis, particularly in the later part of the campaign (Table 4).

We estimated the $\delta^{15}N$ of the fire end-member using our measurements from low fire background periods and mass balance calculations (Table 4). The background at each station was computed separately: 0.11 μgN/m^3 and −4.3‰ at Caribou and 0.07 μgN/m^3 and 1.9‰ at Delta. This approach yielded an average fire $\delta^{15}N$ of 17.0 ± 3.7‰ at Caribou ($n = 4$) and 14.0‰ at Delta ($n = 1$). Combining all of the high fire samples from both stations, we estimated that mean boreal fire $\delta^{15}N$ was 16.4 ± 3.5‰.

In contrast to $\delta^{15}N$, the $\delta^{13}C$ of TC did not vary significantly as a function of time or location (Figures 7e and 7f). The average $\delta^{13}C$ among all samples was −27.2 ± 0.2‰ (Table 4), which corresponds well to the $\delta^{13}C$ composition of boreal forest biomass [*Brooks et al.*, 1997]. The mean $\delta^{13}C$ measured in high fire samples from both sites was the same. We did not attempt to remove a background fraction because of the low variability in the samples.

3.6. Estimating Depth of Burn From Aerosol and Soil Isotope Measurements

In each soil profile, bulk soil carbon density and $\Delta^{14}C$ increased as a function of depth from the surface moss layer to the mesic horizon (Figures 8a and 8b). For the three black spruce profiles the average $\Delta^{14}C$ measured in the surface moss layer was 78‰ ± 13‰, and this increased to 189‰ ± 22‰ for samples collected

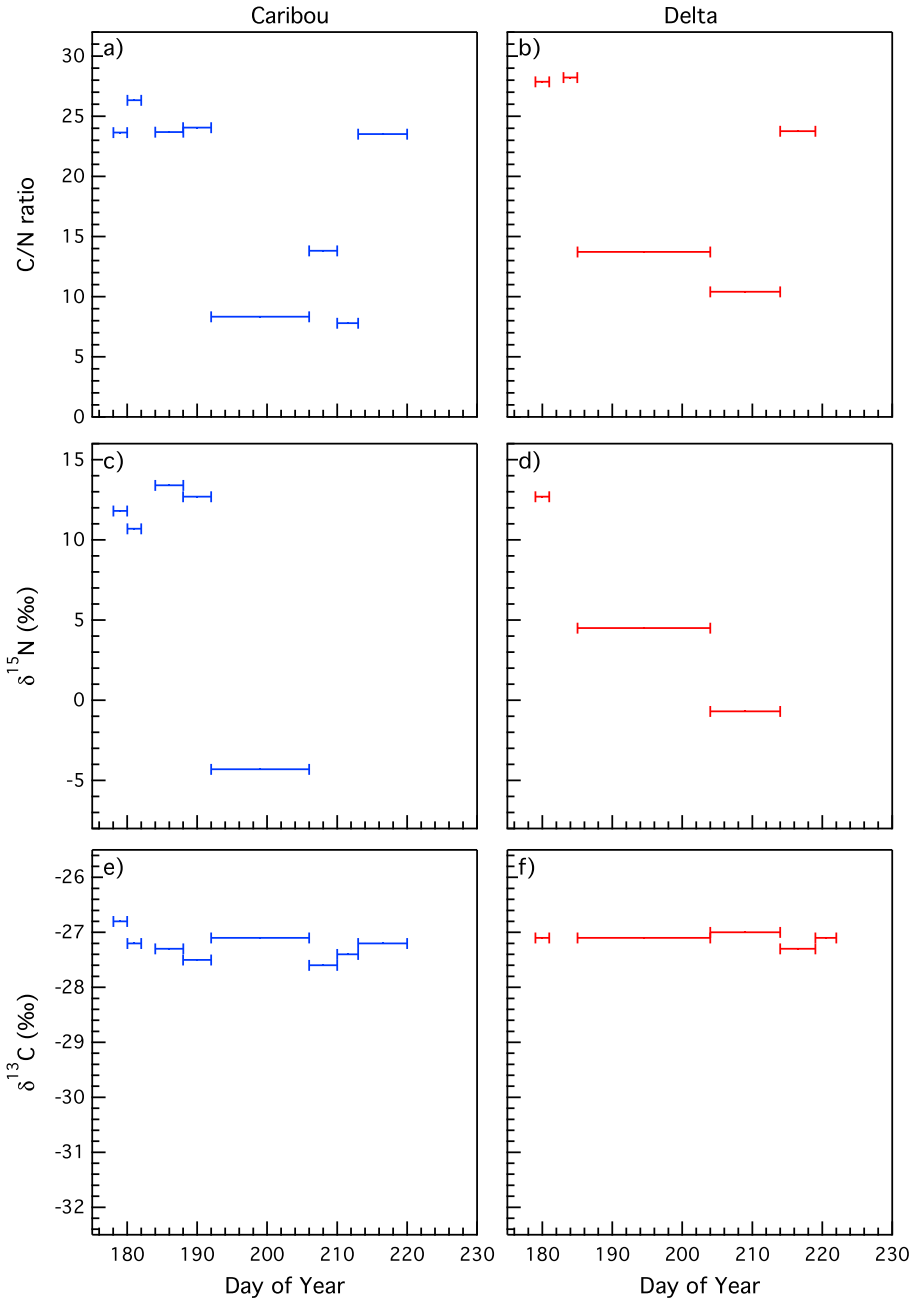

Figure 7. Elemental and stable isotope composition of bulk $PM_{2.5}$. The top row shows (a and b) C/N ratio, while the middle and bottom rows show the stable isotope composition of the aerosols: (c and d) $\delta^{15}N$ and (e and f) $\delta^{13}C$ for Caribou (blue) and Delta (red) stations, respectively.

between 15 cm and 28 cm in the mesic layer. Black spruce ecosystems are the dominant contributor to burned area and carbon emissions in boreal North America [*Rogers et al.*, 2015; *Veraverbeke et al.*, 2015], and combustion of surface soil organic matter horizons is the primary source of ecosystem-level emissions [*Boby et al.*, 2010; *Turetsky et al.*, 2010; *Rogers et al.*, 2014]. The mixed white spruce aspen forest soil profile had thinner organic carbon horizons with lower $\Delta^{14}C$ values (Figures 8a and 8b), which is consistent with more rapid rates of soil carbon turnover at this site [*Flanagan and Van Cleve*, 1983; *Johnstone et al.*, 2010]. Both $\delta^{13}C$ and $\delta^{15}N$ also increased with depth in each soil profile (Figures 8c and 8d). The relatively low $\delta^{13}C$ values in the surface layers (with a mean of -30.5 ± 1.1‰) were consistent with refixation of soil respired CO_2 by surface mosses [*Flanagan et al.*, 1996]. The $\delta^{15}N$ increased from -3.0 ± 0.7‰ in the surface moss layer

Table 4. Elemental and Stable Isotope Analysis of Aerosol Samples[a]

Sample Period	Day of Year	TC ($\mu g\,m^{-3}$)	N ($\mu g\,m^{-3}$)	C/N	C/N Background Corrected	$\delta^{15}N$ (‰)	$\delta^{15}N$ (‰) Background Corrected	$\delta^{13}C$ (‰)
				Caribou				
27–29 Jun[b]	178–180	7.33	0.31	23.6	31.1	11.8	20.8	−26.8
29 Jun 29 to 1Jul[b]	180–182	21.03	0.80	26.3	29.0	10.7	13.2	−27.2
3–7 Jul[b]	184–188	10.20	0.43	23.7	28.4	13.4	19.5	−27.3
7–11 Jul[b]	188–192	26.63	1.11	24.1	25.6	12.7	14.6	−27.5
11–25 Jul[c]	192–206	0.92	0.11	8.3	bkg	−4.3	bkg	−27.1
25–29 Jul[c]	206–210	1.17	0.08	13.8	bkg	-	-	−27.6
29 Jul to 1 Aug[c]	210–213	1.28	0.16	7.8	bkg	-	-	−27.4
1–8 Aug	213–220	3.20	0.14	23.5	82.3	-	-	−27.2
				Delta				
28–30 Jun[b]	179–181	18.82	0.68	27.9	29.7	12.7	14.0	−27.1
2–4 Jul[c]	183–185	0.63	0.02	28.2	bkg	-	-	-
4–23 Jul[c]	185–204	1.21	0.09	13.7	bkg	4.5	bkg	−27.1
23 Jul to 2 Aug[c]	204–214	1.19	0.11	10.4	bkg	−0.7	bkg	−27.0
2–7 Aug	214–219	2.91	0.12	23.8	39.9	-	-	−27.3
7–10 Aug[b]	219–222	4.17	0.11	38.8	96.5	-	-	−27.1

[a]No value is reported if samples were too small to provide reliable isotopic measurements. Where $\delta^{15}N$ was not reported, N concentrations were low and consequently C/N measurements are subject to higher uncertainty.
[b]High fire samples.
[c]Background samples.

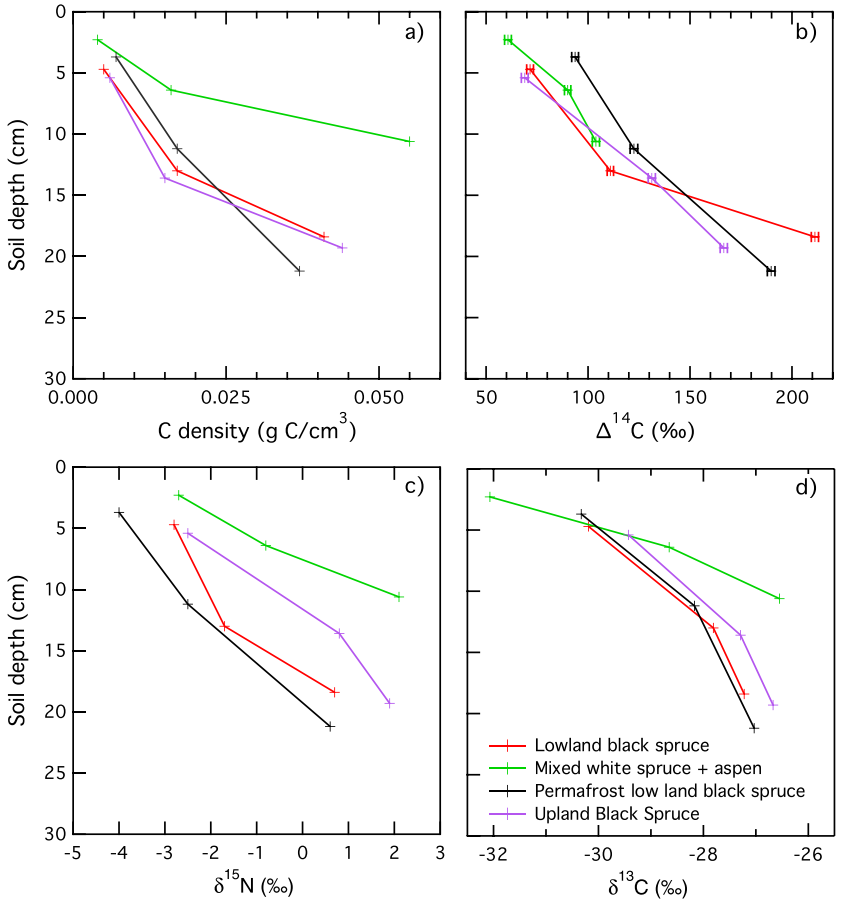

Figure 8. Elemental and isotopic composition of bulk soil organic matter. Soil samples were analyzed for the following soil horizons: mesic, fibric, moss. Each layer was homogenized and results are shown at the average depth of the layers. (a) Carbon density as a function of soil depth, followed by (b) the radiocarbon measurements for each soil core averaged per layer. Stable isotope measurements are shown in the bottom row: (c) $\delta^{15}N$ and (d) $\delta^{13}C$.

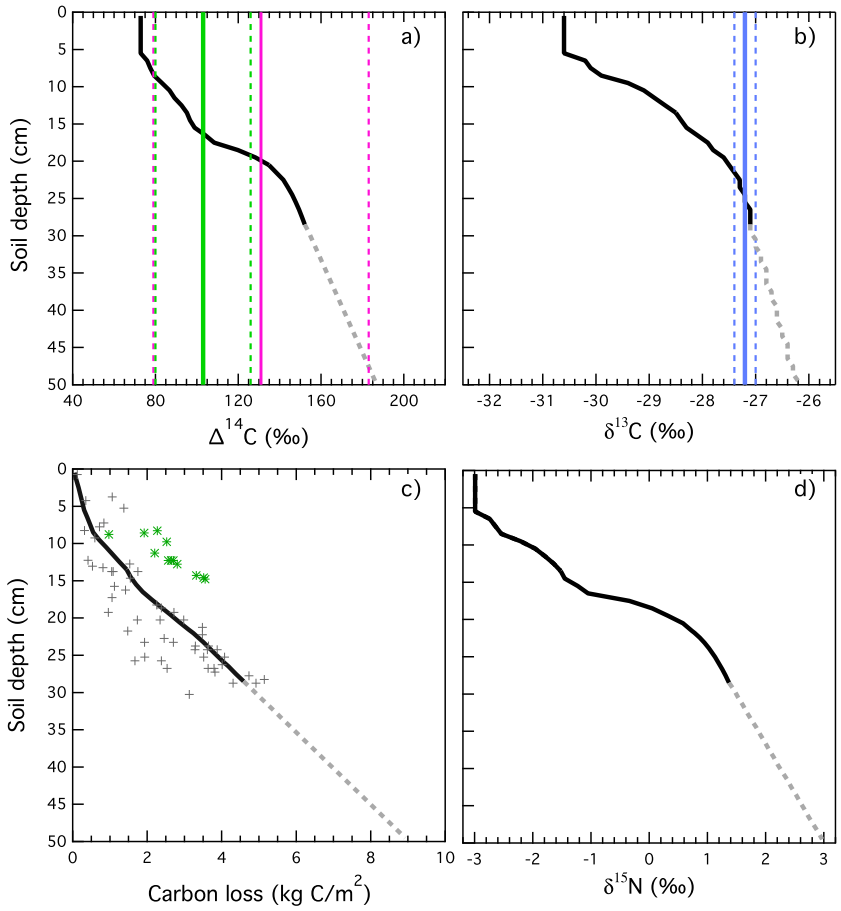

Figure 9. Depth-integrated measurements of (a) radiocarbon, (b) $\delta^{13}C$, (c) carbon loss per m^2 from *Rogers et al.* [2014], and (d) $\delta^{15}N$, calculated as weighted average contribution of black spruce and mixed white spruce aspen forest of all soil cores. Solid black lines represent the weighted averages where soil data were available. We used a linear regression in the mesic layer to extend the estimates deeper in the soil for the purpose of comparing with the aerosol measurements (dashed grey lines). In Figure 9a the vertical pink line shows the $\Delta^{14}C$ of BC, the green line shows $\Delta^{14}C$ of TC, and the dashed lines show the corresponding uncertainty ranges for these aerosol measurements. In Figure 9b the vertical lines denote the $\delta^{13}C$ of the TC and $\pm 1\sigma$ uncertainty estimates. In Figure 9c the grey symbols show black spruce forest estimates and the green symbols show mixed white spruce aspen forest estimates.

to 1.3 ± 0.8‰ for the deepest mesic soil samples, which is consistent with greater recycling and preferential uptake of lighter N by mycorrhizal fungi and plants [*Högberg*, 1997].

We created an average $\Delta^{14}C$ soil profile by assuming that black spruce forests contributed to 70% of regional emissions [*Veraverbeke et al.*, 2015]. We then superimposed the average aerosol $\Delta^{14}C$ to estimate a mean depth of burn consistent with the atmospheric observations, assuming that aboveground components of fuel consumption were small (Figure 9a). The $\Delta^{14}C$ of BC was consistent with a depth of burn of 20 cm and propagating $\pm 1\sigma$ yielded an asymmetrical depth of burn range of 8 cm to 47 cm. Similarly, $\Delta^{14}C$ of TC was consistent with a depth of 16 cm (with a range of 8 to 19 cm), and the average $\delta^{13}C$ of the TC was consistent with a depth of burning of 25 cm (with a range of 21 to 31 cm) (Figure 9b). Pooling all three types of aerosol isotope measurement, we estimated average depth of burn of 20 cm (with a range of 8 cm to 47 cm).

Translating this 20 cm mean depth of burn into carbon loss using the data *Rogers et al.* [2014] yielded a carbon consumption rate of 2.9 kg C m^{-2} (Figure 9c). This value is consistent with reports of average wildfire carbon consumption from soil organic matter layers in black spruce ecosystems between 2.5 and 3.0 kg C m^{-2} [*Kasischke et al.*, 1995; *French et al.*, 2002; *Boby et al.*, 2010; *Rogers et al.*, 2014; *Veraverbeke et al.*, 2015] and provides a mechanistic underpinning of the causes of isotopic variation in boreal fire aerosol.

3.7. Enrichment of Nitrogen Isotopes During Combustion and Atmospheric Processing

Comparison of $\delta^{15}N$ in aerosol during high fire periods with soil $\delta^{15}N$ profiles suggests that there is significant $\delta^{15}N$ discrimination as a consequence of combustion and atmospheric chemical processing. The depth-integrated soil $\delta^{15}N$, weighted for the respective black spruce and mixed white spruce/aspen contributions to emissions, increases with soil depth (Figure 9d). Taking the $\delta^{15}N$ of fire-emitted aerosol ($\delta^{15}N_{aerosol}$) and the burning of soil organic matter as the N source during combustion ($\delta^{15}N_{som}$), we calculated an effective discrimination [e.g., *Högberg*, 1997]:

$$\Delta_{combustion} = \frac{\delta^{15}N_{aerosol} - \delta^{15}N_{som}}{1 + \frac{\delta^{15}N_{som}}{1000}} \cong \delta^{15}N_{aerosol} - \delta^{15}N_{som} \quad (4)$$

Using our background-subtracted estimate of fire-emitted $\delta^{15}N$ (16.4 ± 3.5‰), together with a $\delta^{15}N$ of soil organic matter that corresponded to a depth of 20 cm (0.5‰), we estimated that $\Delta_{combustion}$ was 15.8‰ (±3.5‰). Assuming deeper burning to 30 cm had the effect of reducing this estimate to 14.8‰ (±3.5‰) whereas shallower burning to 10 cm caused an increase to 18.4‰ (±3.5‰). This positive discrimination is consistent with more of the lighter isotopes of N remaining in the gas phase, and pyrodenitrification of organic N to N_2 during combustion [*Kuhlbusch et al*., 1991] preferentially operating on ^{14}N.

4. Discussion

4.1. Constraining Boreal Forest Fire Aerosol Contributions Using Radiocarbon

Quantifying the boreal forest fire contribution to the BC load in the Arctic has relied primarily on chemical transport modeling, based on back trajectory analysis and burned area statistics [e.g., *Stohl et al*., 2006; *Hegg et al*., 2009; *Warneke et al*., 2009] and/or data validation comparison with chemical tracers such as vanilic acid [*McConnell et al*., 2007], ammonium [*Keegan et al*., 2014], and levoglucosan [*Yttri et al*., 2014] in aerosol, snow, or ice samples. The measurements we report here strengthen our capacity to use ^{14}C as a tracer for separating fossil and wildfire contributions to BC deposition in the Arctic. Particularly for aerosols that have a significant modern fraction, an improved boreal forest fire end-member can help reduce uncertainties in source apportionment.

In past work, the $\Delta^{14}C$ signature of the biomass burning end-member has often been assigned using poorly quantified assumptions about the relative age of the biomass combusted, which varies significantly between fuels, ecosystems, and regions. The biomass burning end-member is sometimes reported as a range between recently assimilated biomass (that has the same $\Delta^{14}C$ as atmospheric CO_2) and wood for which an age distribution is prescribed (Table 1). For wildland fires in boreal forests, particularly in North America and especially in Alaska, this approach is problematic because the primary fuel consumed by fires is soil organic matter that has accumulated over a period of several decades [*Boby et al*., 2010; *Rogers et al*., 2014]. By directly quantifying the $\Delta^{14}C$ of fire-emitted aerosol, we address this problem for boreal fires and report for the first time direct measurements of the $\Delta^{14}C$ signature of boreal fire-derived BC, TC, and OC.

The true $\Delta^{14}C$ signature for biomass burning evolves through time as a result of the changing atmospheric $\Delta^{14}CO_2$ time series and the age of the organic material that is being combusted (e.g., Figure 6). While most of the studies listed in Table 1 use similar approaches when determining the biomass end-member, only one reports direct measurements of the biomass burning end-member: *Klinedinst and Currie* [1999] measured the $\Delta^{14}C$ of TC from the combustion of softwood and hardwood in $PM_{2.5}$ emissions. After correcting for changing levels of atmospheric $\Delta^{14}C$, the relative age of softwood reported by *Klinedinst and Currie* [1999] of 19 to 21 years is in good agreement with our mean BC age estimate of 20 years, yet the origin of the combusted pool is fundamentally different. Wood burning in many cities in North America may primarily consist of tree branches and boles, whereas for boreal forest fires the predominant carbon source is organic soils. The 11 to 47 year age range we report for BC takes into account different contributions of individual fires and background variations at our two stations and is larger than the 16 to 28 year range reported by *Klinedinst and Currie* [1999].

Boreal-fire-derived BC measured at Caribou was older than the fire-emitted OC at this site when estimated using either the Keeling Plot or background removal approach (Table 3). Although differences between these components were not observed at Delta, the age difference at Caribou suggests that under some conditions

BC and OC aerosol production may be sensitive to different aspects of fire behavior. Flaming fires, in contrast to smoldering fires, lead to a more complete combustion and more BC production [*Reid et al*., 2005; *Yokelson et al*., 2013]. In boreal forests, higher BC/OC ratios reported during flaming fires [*Mazurek et al*., 1991; *Conny and Slater*, 2002] also may correspond to periods when atmospheric conditions are drier, enabling more complete combustion of small stems, branches, and deeper organic layers. If these fuels are older than fuels consumed during smoldering phases, then BC would be expected to have more positive $\Delta^{14}C$ values. To test this hypothesis, and whether BC and OC age differences are robust, higher-resolution measurements are needed in close proximity to large boreal wildfires, preferably during contrasting periods of fire weather promoting smoldering and flaming fire behavior.

4.2. Fire-Climate Feedbacks and Implication for the Arctic

Reducing uncertainties in BC loading, deposition, and source attribution is particularly important in the Arctic during summer months, where BC climate feedbacks are most active [e.g., *Sharma*, 2004; *Bond et al*., 2013; *Keegan et al*., 2014]. Here we demonstrate that boreal fires in Alaska are a main source of BC in summer in a year with average burning. Over the past five decades, large fire years in Alaska have become more frequent [*Kasischke et al*., 2010; *Kelly et al*., 2013]. *Turetsky et al*. [2010] showed that in Alaska, ground layer combustion has accelerated regional carbon losses over the past decade, owing to increases in burn area and late-season burning. With the wildfire season expected to become longer and more intense [*Amiro et al*., 2009; *Balshi et al*., 2009; *de Groot et al*., 2013; *Flannigan et al*., 2013], the BC contribution to the Arctic climate feedbacks would also be expected to increase.

One possible outcome is that the likelihood of widespread melt events like the one observed in Greenland by *Keegan et al.* [2014] may increase, especially if fire plumes are injected high enough into the free troposphere. *Val Martin et al*. [2010] observed a positive correlation between MODIS-detected fire radiative power and plume heights, indicating that higher plumes are the result of higher fire intensity. Under current prediction of increased boreal fire intensity [*de Groot et al*., 2013; *Flannigan et al*., 2013] one can expect deeper burning constituting more emissions and higher injection heights, thus increasing the likelihood for aerosol deposition in remote areas of the Arctic. These interactions highlight the need for future work to better understand how a changing boreal fire regime influences BC emissions and deposition.

As ^{14}C becomes more widely used for BC source attribution, our estimates may reduce uncertainties in BC source apportionment in the Arctic. An important future step will be to use the recent methodological improvements and the end-member data described here to quantify the contribution of boreal fires in Alaska to the BC loading and deposition in different areas of the Arctic. Using remote measurements to constrain models will improve our capacity to quantify and predict future climate forcing from BC.

4.3. Influence of Depth of Burn on Aerosol Isotopic Composition

Another important implication of this study is the possible use of aerosol $\Delta^{14}C$ and soil isotope profiles to infer information about the depth of burning into the organic soils. Soil organic matter in Alaskan boreal forests is known to comprise the vast majority of carbon losses emitted during fuel consumption [*Dyrness and Norum*, 1983; *Kasischke et al*., 1995; *French et al*., 2002; *Veraverbeke et al*., 2015]. Since surface fires and subsequent smoldering in Alaskan black spruce forests can consume the ground layer biomass down to the mineral soil, with an average consumption of 40–60% of the biomass in the soil organic horizons [*Dyrness and Norum*, 1983; *Kasischke et al*., 1995], the propagation of the ^{14}C bomb spike into these horizons can provide information about the contribution of different layers to the overall fuel consumption. A possible advantage of an aerosol-based approach is that remote air sampling may enable averaging over wide range of climate and landscape characteristics that are known to influence field measurements of fuel consumption [*French*, 2004; *Kane et al*., 2007; *Turetsky et al*., 2011].

We used our isotope measurements of fire-emitted BC in the summer of 2013, together with soil profile measurements near the 2010 Gilles Creek fire perimeter to estimate a mean depth of burn of 20 cm and a range from 8 to 47 cm (Figure 9). In comparison, the AKFED-estimated average depth of burning in black spruce ecosystems for 2013 was 13 cm with a standard deviation of 4 cm. While our estimate of depth of burn is higher than the AKFED model prediction, the two estimates agree within known uncertainties. The depth of burn reported by *Rogers et al*. [2014] for the Gilles Creek fire ranged between 1 and 30 cm, with a mean of 19 cm in black spruce ecosystems, which also is consistent with our mean estimate. Our study provides

evidence that the carbon isotopic composition of aerosols emitted by boreal fires is significantly influenced by the depth of burn in organic soils.

Quantitative use of aerosols to reduce uncertainties in boreal fuel consumption may be possible but would require more extensive atmospheric and soil isotopic sampling. High temporal resolution aerosol sampling during a high fire year, however, has the potential to immediately test if the depth of burning becomes progressively deeper through the fire season as a consequence of a thickening active layer and improved drainage of deeper soil horizons [*Soja*, 2004; *Turetsky et al*., 2011; *Kasischke and Hoy*, 2012; *Veraverbeke et al*., 2015]. If this mechanism is important at a regional scale, we would expect increasing levels of $\Delta^{14}C$, $\delta^{13}C$, and $\delta^{15}N$ of fire aerosol as the fire season progresses. If other processes dominate, however, including seasonal changes in burning among different vegetation types or controls by synoptic-scale variations in fire weather, we would expect other patterns to emerge in the aerosol isotope tracers.

4.4. Nitrogen Isotope Discrimination During Combustion

The $\delta^{15}N$ in aerosols exhibited significant enrichment during high fire periods that is likely associated with discrimination during combustion and atmospheric chemistry processes. High $\delta^{15}N$ in aerosols has been observed in other studies [*Kundu et al*., 2010; *Aggarwal et al*., 2013; *Mkoma et al*., 2014; *Pavuluri et al*., 2015], but the pathways responsible for the more positive $\delta^{15}N$ measured in aerosols are not fully understood. *Turekian et al*. [1998] reported $\delta^{15}N$ range of particular matter produced by biomass burning of tropical C3 plants of 2.0‰ to 19.5‰ in a laboratory setting. The observed discrimination during the combustion process with respect to the $\delta^{15}N$ of the plant material ranged from −1.3 to 13.1‰. *Turekian et al*. [1998] further suggested that different nitrogenous compounds are accessed at different temperatures of heating, which could explain some of the variability in our measurements. Other studies suggest that the isotopic enrichment of ^{15}N is associated with atmospheric processing of aerosols, in particular, gas to particle conversion of NH_3 and NO_x [*Pavuluri et al*., 2010; *Aggarwal et al*., 2013].

Studies have reported $\delta^{15}N$ data for aerosols derived from different combustion sources such as diesel (4.6 ± 0.8‰), natural gas (7.7 ± 5.9‰), fuel oil (−7.5 ± 8.3‰), coal (−5.3‰), and unleaded gasoline (average 4.6‰, ranging from −16 to 16‰) [*Widory*, 2007]. Our study presents the first measurements indicating the presence of $\delta^{15}N$ discrimination for fire-emitted aerosols in boreal forest ecosystems and provides evidence for discrimination levels that exceed observations from the other systems.

Acknowledgments
A portion of the research described in this paper was performed for the Carbon in Arctic Reservoirs Vulnerability Experiment (CARVE), an Earth Ventures (EV-1) investigation, under contract with the National Aeronautics and Space Administration. This work was also supported by a generous gift from the Jenkins Family (to C.I.C.). We would like to thank Jamie Hollingsworth from the Bonanza Creek Long-Term Ecological Research (LTER) program and Alan Tonne from the University of Alaska Fairbanks Experiment Farm, who provided invaluable help in setting up the aerosol sampling stations for the campaign. We used data obtained from IMPROVE—a collaborative association of state, tribal, and federal agencies, and international partners (U.S. Environmental Protection Agency is the primary funding source, with contracting and research support from the National Park Service). We would also like to thank the colleagues from the University of California, Irvine, and the undergraduate students Nicolas Cuozzo and Ashley Braunthal who helped collect data as part of the NSF Research Experience for Undergraduate (REU) program.

5. Conclusions

We measured BC concentration together with isotopic and elemental composition of bulk aerosols in interior Alaska in the summer of 2013 during periods with high and low boreal forest fire activity. Our measurements agree with atmospheric transport model predictions and IMPROVE network observations, indicating that boreal fire emissions were a significant driver of BC and OC aerosol variability in Alaska during a year with average burning. We also measured the radiocarbon content of BC, thus being the first study to directly constrain the $\Delta^{14}C$ end-member of boreal fire-emitted BC. The fire-emitted $\Delta^{14}C$ signature of BC may help quantify the boreal fire contribution to the BC load in the Arctic under a changing boreal fire regime and reduce uncertainties in BC source apportionment studies. Our analysis of the elemental and isotopic composition of aerosols shows that the depth of burn in soil organic matter layers significantly influences aerosol composition. Combining $\Delta^{14}C$ and $\delta^{13}C$ analysis of aerosols with soil profile observations in future work may provide a constraint on spatial and temporal variations in the depth of burn and fuel consumption in boreal forest ecosystems.

References

Ackerman, A., O. Toon, J. Taylor, D. Johnson, P. Hobbs, and R. Ferek (2000), Effects of aerosols on cloud albedo: Evaluation of Twomey's parameterization of cloud susceptibility using measurements of ship tracks, *J. Atmos. Sci.*, *1995*, 2684–2695.

Aggarwal, S. G., K. Kawamura, G. S. Umarji, E. Tachibana, R. S. Patil, and P. K. Gupta (2013), Organic and inorganic markers and stable C-, N-isotopic compositions of tropical coastal aerosols from megacity Mumbai: Sources of organic aerosols and atmospheric processing, *Atmos. Chem. Phys.*, *13*, 4667–4680, doi:10.5194/acp-13-4667-2013.

Akagi, S. K., R. J. Yokelson, C. Wiedinmyer, M. J. Alvarado, J. S. Reid, T. Karl, J. D. Crounse, and P. O. Wennberg (2011), Emission factors for open and domestic biomass burning for use in atmospheric models, *Atmos. Chem. Phys.*, *11*, 4039–4072, doi:10.5194/acp-11-4039-2011.

Amiro, B. D., et al. (2006), The effect of post-fire stand age on the boreal forest energy balance, *Agric. For. Meteorol.*, *140*(1–4), 41–50, doi:10.1016/j.agrformet.2006.02.014.

Amiro, B. D., A. S. Cantin, M. D. Flannigan, and W. J. de Groot (2009), Future emissions from Canadian boreal forest fires, *Can. J. For. Res.*, *39*(2), 383–395, doi:10.1139/X08-154.

Andreae, M. O., T. W. Andreae, R. Ferek, and H. Raemdonck (1984), Long-range transport of soot carbon in the marine atmosphere, *Sci. Total Environ.*, *36*, 73–80, doi:10.1016/0048-9697(84)90249-3.

Balshi, M. S., A. D. Mcguire, P. Duffy, M. Flannigan, D. W. Kicklighter, and J. Melillo (2009), Vulnerability of carbon storage in North American boreal forests to wildfires during the 21st century, *Global Change Biol.*, *15*(6), 1491–1510, doi:10.1111/j.1365-2486.2009.01877.x.

Bauer, S. E., S. Menon, D. Koch, T. C. Bond, and K. Tsigaridis (2010), A global modeling study on carbonaceous aerosol microphysical characteristics and radiative effects, *Atmos. Chem. Phys.*, *10*(15), 7439–7456, doi:10.5194/acp-10-7439-2010.

Bench, G. (2004), Measurement of contemporary and fossil carbon contents of $PM_{2.5}$ aerosols: Results from Turtleback Dome, Yosemite National Park, *Environ. Sci. Technol.*, *38*(8), 2424–2427.

Bench, G., S. Fallon, B. Schichtel, W. Malm, and C. McDade (2007), Relative contributions of fossil and contemporary carbon sources to $PM_{2.5}$ aerosols at nine Interagency Monitoring for Protection of Visual Environments (IMPROVE) network sites, *J. Geophys. Res.*, *112*, D10205, doi:10.1029/2006JD007708.

Bernardoni, V., et al. (2013), Radiocarbon analysis on organic and elemental carbon in aerosol samples and source apportionment at an urban site in Northern Italy, *J. Aerosol Sci.*, *56*, 88–99, doi:10.1016/j.jaerosci.2012.06.001.

Boby, L. A., E. A. G. Schuur, M. C. Mack, D. Verbyla, and J. F. Johnstone (2010), Quantifying fire severity, carbon, and nitrogen emissions in Alaska's boreal forest, *Ecol. Appl.*, *20*(6), 1633–1647, doi:10.1890/08-2295.1.

Bonan, G. B. (2008), Forests and climate change: Forcings, feedbacks, and the climate benefits of forests, *Science*, *320*(5882), 1444–1449, doi:10.1126/science.1155121.

Bond, T. C., et al. (2013), Bounding the role of black carbon in the climate system: A scientific assessment, *J. Geophys. Res. Atmos.*, *118*, 5380–5552, doi:10.1002/jgrd.50171.

Boulanger, Y., S. Gautheir, and P. J. Burton (2014), A refinement of models projecting future Canadian fire regimes using homogeneous fire regime zones, *Can. J. For. Res.*, *376*, 1–44, doi:10.1139/cjfr-2013-0372.

Bowman, D. M. J. S., et al. (2009), Fire in the Earth system, *Science*, *324*(5926), 481–484, doi:10.1126/science.1163886.

Brooks, J. R., L. B. Flanagan, N. Buchmann, and J. R. Ehleringer (1997), Carbon isotope composition of boreal plants: Functional groupings of life forms, *Oecologia*, *110*, 301–311.

Carrasco, J. J., J. C. Neff, and J. W. Harden (2006), Modeling physical and biogeochemical controls over carbon accumulation in a boreal forest soil, *J. Geophys. Res.*, *111*, G02004, doi:10.1029/2005JG000087.

Chen, B., et al. (2013), Source forensics of black carbon aerosols from China, *Environ. Sci. Technol.*, *47*, 9102–9108, doi:10.1021/es401599r.

Chen, Y., Q. Li, J. T. Randerson, E. A. Lyons, R. A. Kahn, D. L. Nelson, and D. J. Diner (2009), The sensitivity of CO and aerosol transport to the temporal and vertical distribution of North American boreal fire emissions, *Atmos. Chem. Phys.*, *2*, 6559–6580.

Chow, J. C., J. G. Watson, L. W. A. Chen, M. C. O. Chang, N. F. Robinson, D. Trimble, and S. Kohl (2007), The IMPROVE_A temperature protocol for thermal/optical carbon analysis: Maintaining consistency with a long-term database, *J. Air Waste Manage. Assoc.*, *57*(9), 1014–1023, doi:10.3155/1047-3289.57.9.1014.

Conny, J. M., and J. F. Slater (2002), Black carbon and organic carbon in aerosol particles from crown fires in the Canadian boreal forest, *J. Geophys. Res.*, *107*(D11), 4116, doi:10.1029/2001JD001528.

Cozic, J., B. Verheggen, S. Mertes, P. Connolly, K. Bower, A. Petzold, U. Baltensperger, and E. Weingartner (2007), Scavenging of black carbon in mixed phase clouds at the high alpine site Jungfraujoch, *Atmos. Chem. Phys.*, *7*(7), 1797–1807, doi:10.5194/acp-7-1797-2007.

Croft, B., U. Lohmann, and K. Von Salzen (2005), Black carbon ageing in the Canadian Centre for Climate modelling and analysis atmospheric general circulation model, *Atmos. Chem. Phys.*, *5*, 1931–1949.

Damoah, R., N. Spichtinger, R. Servranckx, M. Fromm, E. W. Eloranta, I. A. Razenkov, P. James, M. Shulski, C. Forster, and A. Stohl (2006), A case study of pyro-convection using transport model and remote sensing data, *Atmos. Chem. Phys.*, *6*(1), 173–185, doi:10.5194/acp-6-173-2006.

Davis, A. Y., et al. (2015), Fire emission uncertainties and their effect on smoke dispersion predictions: A case study at Eglin Air Force Base, *Int. J. Wildland Fire*, *24*, 276–285.

De Groot, W. J., M. D. Flannigan, and A. S. Cantin (2013), Climate change impacts on future boreal fire regimes, *For. Ecol. Manage.*, *294*, 35–44, doi:10.1016/j.foreco.2012.09.027.

Doherty, S. J., S. G. Warren, T. C. Grenfell, A. D. Clarke, and R. E. Brandt (2010), Light-absorbing impurities in Arctic snow, *Atmos. Chem. Phys.*, *10*(23), 11,647–11,680, doi:10.5194/acp-10-11647-2010.

Dyrness, C., and R. Norum (1983), The effects of experimental fires on black spruce forest floors in interior Alaska, *Can. J. For. Res.*, *13*, 879–893.

Euskirchen, E. S., A. D. McGuire, T. S. Rupp, F. S. Chapin, and J. E. Walsh (2009), Projected changes in atmospheric heating due to changes in fire disturbance and the snow season in the western Arctic, 2003–2100, *J. Geophys. Res.*, *114*, G04022, doi:10.1029/2009JG001095.

Flanagan, L. B., J. R. Brooks, G. T. Varney, S. C. Berry, and J. R. Ehleringer (1996), Carbon isotope discrimination during photosynthesis and the isotope ratio of respired CO_2 in boreal forest ecosystems, *Global Biogeochem. Cycles*, *10*, 629–640, doi:10.1029/96GB02345.

Flanagan, P. W., and K. Van Cleve (1983), Nutrient cycling in relation to decomposition and organic-matter quality in taiga ecosystems, *Can. J. For. Res.*, *13*, 795–817, doi:10.1139/x83-110.

Flanner, M. G., C. S. Zender, J. T. Randerson, and P. J. Rasch (2007), Present-day climate forcing and response from black carbon in snow, *J. Geophys. Res.*, *112*, D11202, doi:10.1029/2006JD008003.

Flanner, M. G., C. S. Zender, P. G. Hess, N. M. Mahowald, T. H. Painter, V. Ramanathan, and P. J. Rasch (2009), Springtime warming and reduced snow cover from carbonaceous particles, *Atmos. Chem. Phys.*, *9*(7), 2481–2497, doi:10.5194/acp-9-2481-2009.

Flannigan, M., A. S. Cantin, W. J. de Groot, M. Wotton, A. Newbery, and L. M. Gowman (2013), Global wildland fire season severity in the 21st century, *For. Ecol. Manage.*, *294*, 54–61, doi:10.1016/j.foreco.2012.10.022.

Forster, C., et al. (2001), Transport of boreal forest fire emissions from Canada to Europe, *J. Geophys. Res.*, *106*(D19), 22,887–22,906, doi:10.1029/2001JD900115.

French, N. H. F. (2004), Uncertainty in estimating carbon emissions from boreal forest fires, *J. Geophys. Res.*, *109*, D14S08, doi:10.1029/2003JD003635.

French, N. H. F., E. S. Kasischke, and D. G. Williams (2002), Variability in the emission of carbon-based trace gases from wildfire in the Alaskan boreal forest, *J. Geophys. Res.*, *108*(D1), 8151, doi:10.1029/2001JD000480.

French, N. H. F., et al. (2011), Model comparisons for estimating carbon emissions from North American wildland fire, *J. Geophys. Res.*, *116*, G00K05, doi:10.1029/2010JG001469.

Fromm, M. (2005), Pyro-cumulonimbus injection of smoke to the stratosphere: Observations and impact of a super blowup in northwestern Canada on 3–4 August 1998, *J. Geophys. Res.*, *110*, D08205, doi:10.1029/2004JD005350.

Gelencser, A. (2004), in *Carbonaceous Aerosol*, edited by K. Mysak and L. A. Hamilton, Springer, Netherlands.

Gelencsér, A., B. May, D. Simpson, A. Sánchez-Ochoa, A. Kasper-Giebl, H. Puxbaum, A. Caseiro, C. A. Pio, and M. Legrand (2007), Source apportionment of $PM_{2.5}$ organic aerosol over Europe: Primary/secondary, natural/anthropogenic, and fossil/biogenic origin, *J. Geophys. Res.*, *112*, D23S04, doi:10.1029/2006JD008094.

Ghan, S. J., X. Liu, R. C. Easter, R. Zaveri, P. J. Rasch, J. H. Yoon, and B. Eaton (2012), Toward a minimal representation of aerosols in climate models: Comparative decomposition of aerosol direct, semidirect, and indirect radiative forcing, *J. Clim.*, *25*(19), 6461–6476, doi:10.1175/JCLI-D-11-00650.1.

Gonfiantini, R. (1984), Advisory group meeting on stable isotope reference samples for geochemical and hydrological investigations, *IAEA, Vienna 19–21 Sept. 1983. Rep. to Dir. Gen.*, 77.

Gustafsson, O., M. Kruså, Z. Zencak, R. J. Sheesley, L. Granat, E. Engström, P. S. Praveen, P. S. P. Rao, C. Leck, and H. Rodhe (2009), Brown clouds over South Asia: Biomass or fossil fuel combustion?, *Science*, *323*(5913), 495–498, doi:10.1126/science.1164857.

Hadley, O. L., and T. W. Kirchstetter (2012), Black-carbon reduction of snow albedo, *Nat. Clim. Change*, *2*(6), 437–440, doi:10.1038/nclimate1433.

Hansen, J., and L. Nazarenko (2004), Soot climate forcing via snow and ice albedos, *Proc. Natl. Acad. Sci. U.S.A.*, *101*(2), 423–428, doi:10.1073/pnas.2237157100.

Hansen, J., M. Sato, R. Ruedy, A. Lacis, and V. Oinas (2000), Global warming in the twenty-first century: An alternative scenario, *Proc. Natl. Acad. Sci. U.S.A.*, *97*(18), 9875–9880, doi:10.1073/pnas.170278997.

Heal, M. R., P. Naysmith, G. T. Cook, S. Xu, T. R. Duran, and R. M. Harrison (2011), Application of 14C analyses to source apportionment of carbonaceous $PM_{2.5}$ in the UK, *Atmos. Environ.*, *45*(14), 2341–2348, doi:10.1016/j.atmosenv.2011.02.029.

Hegg, D. A., S. G. Warren, T. C. Grenfell, S. J. Doherty, T. V. Larson, and A. D. Clarke (2009), Source attribution of black carbon in Arctic snow, *Environ. Sci. Technol.*, *43*(11), 4016–4021.

Hegg, D. A., S. G. Warren, T. C. Grenfell, and A. D. Clarke (2010), Sources of light-absorbing aerosol in arctic snow and their seasonal variation, *Atmos. Chem. Phys.*, *10*(22), 10,923–10,938, doi:10.5194/acp-10-10923-2010.

Henderson, J. M., et al. (2015), Atmospheric transport simulations in support of the Carbon in Arctic Reservoirs Vulnerability Experiment (CARVE), *Atmos. Chem. Phys.*, *15*(8), 4093–4116, doi:10.5194/acp-15-4093-2015.

Högberg, P. (1997), 15 N natural abundance in soil-plant systems, *New Phytol.*, *137*(95), 179–203.

Jacobson, M. Z. (2001), Strong radiative heating due to the mixing state of black carbon in atmospheric aerosols, *Nature*, *409*(6821), 695–697, doi:10.1038/35055518.

Jiao, C., et al. (2014), An AeroCom assessment of black carbon in Arctic snow and sea ice, *Atmos. Chem. Phys.*, *14*(5), 2399–2417, doi:10.5194/acp-14-2399-2014.

Jin, Y., J. T. Randerson, S. J. Goetz, P. S. A. Beck, M. M. Loranty, and M. L. Goulden (2012), The influence of burn severity on postfire vegetation recovery and albedo change during early succession in North American boreal forests, *J. Geophys. Res.*, *117*, G01036, doi:10.1029/2011JG001886.

Johnstone, J. F., F. S. Chapin, T. N. Hollingsworth, M. C. Mack, V. Romanovsky, and M. Turetsky (2010), Fire, climate change, and forest resilience in interior Alaska This article is one of a selection of papers from The Dynamics of Change in Alaska's Boreal Forests: Resilience and Vulnerability in Response to Climate Warming, *Can. J. For. Res.*, *40*, 1302–1312, doi:10.1139/X10-061.

Kahn, R. A., Y. Chen, D. L. Nelson, F.-Y. Leung, Q. Li, D. J. Diner, and J. A. Logan (2008), Wildfire smoke injection heights: Two perspectives from space, *Geophys. Res. Lett.*, *35*, L04809, doi:10.1029/2007GL032165.

Kane, E. S., E. S. Kasischke, D. W. Valentine, M. R. Turetsky, and A. D. McGuire (2007), Topographic influences on wildfire consumption of soil organic carbon in interior Alaska: Implications for black carbon accumulation, *J. Geophys. Res.*, *112*, G03017, doi:10.1029/2007JG000458.

Kasischke, E. S., and E. E. Hoy (2012), Controls on carbon consumption during Alaskan wildland fires, *Global Change Biol.*, *18*(2), 685–699, doi:10.1111/j.1365-2486.2011.02573.x.

Kasischke, E. S., et al. (2010), Alaska's changing fire regime—Implications for the vulnerability of its boreal forests This article is one of a selection of papers from The Dynamics of Change in Alaska's Boreal Forests: Resilience and Vulnerability in Response to Climate Warming, *Can. J. For. Res.*, *40*(7), 1313–1324, doi:10.1139/X10-098.

Kasischke, E., N. C. Jr, and B. Stocks (1995), Fire, global warming, and the carbon balance of boreal forests, *Ecol. Appl.*, *5*(2), 437–451.

Keegan, K. M., M. R. Albert, J. R. McConnell, and I. Baker (2014), Climate change and forest fires synergistically drive widespread melt events of the Greenland Ice Sheet., *Proc. Natl. Acad. Sci. U.S.A.*, *111*(22), 1–4, doi:10.1073/pnas.1405397111.

Kelly, R., M. L. Chipman, P. E. Higuera, I. Stefanova, L. B. Brubaker, and F. S. Hu (2013), Recent burning of boreal forests exceeds fire regime limits of the past 10,000 years, *Proc. Natl. Acad. Sci. U.S.A.*, *110*(32), 13,055–13,060, doi:10.1073/pnas.1305069110.

Klinedinst, D. B., and L. A. Currie (1999), Direct quantification of $PM_{2.5}$ fossil and biomass carbon within the northern front range air quality study's domain, *Environ. Sci. Technol.*, *33*(23), 4146–4154, doi:10.1021/es990355m.

Koch, D., and A. D. Del Genio (2010), Black carbon semi-direct effects on cloud cover: Review and synthesis, *Atmos. Chem. Phys.*, *10*(16), 7685–7696, doi:10.5194/acp-10-7685-2010.

Koch, D., M. Schulz, S. Kinne, C. Mcnaughton, J. R. Spackman, Y. Balkanski, S. Bauer, and T. Berntsen (2009), Evaluation of black carbon estimations in global aerosol models, *Atmos. Chem. Phys.*, *9*, 9001–9026.

Kuhlbusch, T. A., J. M. Lobert, P. J. Crutzen, and P. Warneck (1991), Molecular nitrogen emissions from denitrification during biomass burning, *Nature*, *351*(6322), 135–137, doi:10.1038/351135a0.

Kukavskaya, E. A., A. J. Soja, A. P. Petkov, E. I. Ponomarev, G. A. Ivanova, and S. G. Conard (2013), Fire emissions estimates in Siberia: Evaluation of uncertainties in area burned, land cover, and fuel consumption, *Can. J. For. Res.*, *43*, 493–506.

Kundu, S., K. Kawamura, T. W. Andreae, A. Hoffer, and M. O. Andreae (2010), Diurnal variation in the water-soluble inorganic ions, organic carbon and isotopic compositions of total carbon and nitrogen in biomass burning aerosols from the LBA-SMOCC campaign in Rondônia, Brazil, *J. Aerosol Sci.*, *41*(1), 118–133, doi:10.1016/j.jaerosci.2009.08.006.

Lee, Y. H., et al. (2013), Evaluation of preindustrial to present-day black carbon and its albedo forcing from Atmospheric Chemistry and Climate Model Intercomparison Project (ACCMIP), *Atmos. Chem. Phys.*, *13*(5), 2607–2634, doi:10.5194/acp-13-2607-2013.

Levin, I., T. Naegler, B. Kromer, M. Diehl, R. J. Francey, A. J. Gomez-Pelaez, L. P. Steele, D. Wagenbach, R. Weller, and D. E. Worthy (2010), Observations and modelling of the global distribution and long-term trend of atmospheric $^{14}CO_2$, *Tellus B*, *62*(1), 26–46, doi:10.1111/j.1600-0889.2009.00446.x.

Levine, J. S., and W. R. Cofer (2000), Boreal forest fire emissions and the chemistry of the atmosphere, in *Fire, Climate Change, and Carbon Cycling in the Boreal Forest*, edited by E. S. Kasischke and B. J. Stocks, pp. 31–49, Springer, New York.

Lewis, C. W., G. A. Klouda, and W. D. Ellenson (2004), Radiocarbon measurement of the biogenic contribution to summertime PM-2.5 ambient aerosol in Nashville, TN, *Atmos. Environ.*, *38*(35), 6053–6061, doi:10.1016/j.atmosenv.2004.06.011.

Liousse, C., J. E. Penner, C. Chuang, J. J. Walton, H. Eddleman, and H. Cachier (1996), A global three-dimensional model study of carbonaceous aerosols, *J. Geophys. Res.*, *101*(D14), 19,411–19,432, doi:10.1029/95JD03426.

Liu, H. (2005), Changes in the surface energy budget after fire in boreal ecosystems of interior Alaska: An annual perspective, *J. Geophys. Res.*, *110*, D13101, doi:10.1029/2004JD005158.
Liu, H., and J. T. Randerson (2008), Interannual variability of surface energy exchange depends on stand age in a boreal forest fire chronosequence, *J. Geophys. Res.*, *113*, G01006, doi:10.1029/2007JG000483.
Lohmann, U., and J. Feichter (2005), Global indirect aerosol effects: A review, *Atmos. Chem. Phys.*, *5*, 715–737.
Malm, W., and J. Sisler (1994), Spatial and seasonal trends in particle concentration and optical extinction in the United States, *J. Geophys. Res.*, *99*, 1347–1370, doi:10.1029/93JD02916.
Marks, A. A., and M. D. King (2013), The effects of additional black carbon on the albedo of Arctic sea ice: Variation with sea ice type and snow cover, *Cryosphere*, *7*(4), 1193–1204, doi:10.5194/tc-7-1193-2013.
Mazurek, M. A., W. R. I. Cofer, and J. S. Levine (1991), Carbonaceous aerosols from prescribed burning of a boreal forest ecosystem, in *Global Biomass Burning—Atmospheric, Climatic, and Biospheric Implications*, edited by J. S. Levine, pp. 258–263, MIT, Press, Cambridge, Mass.
McConnell, J. R., R. Edwards, G. L. Kok, M. G. Flanner, C. S. Zender, E. S. Saltzman, J. R. Banta, D. R. Pasteris, M. M. Carter, and J. D. W. Kahl (2007), 20th-century industrial black carbon emissions altered Arctic climate forcing, *Science*, *317*(5843), 1381–1384, doi:10.1126/science.1144856.
McGuire, A. D., F. S. Chapin, J. E. Walsh, and C. Wirth (2006), Integrated regional changes in arctic climate feedbacks: Implications for the Global Climate System *, *Annu. Rev. Environ. Resour.*, *31*(1), 61–91, doi:10.1146/annurev.energy.31.020105.100253.
Minguillón, M. C., et al. (2011), Fossil versus contemporary sources of fine elemental and organic carbonaceous particulate matter during the DAURE campaign in Northeast Spain, *Atmos. Chem. Phys.*, *11*, 12,067–12,084, doi:10.5194/acp-11-12067-2011.
Mkoma, S., K. Kawamura, E. Tachibana, and P. Fu (2014), Stable carbon and nitrogen isotopic compositions of tropical atmospheric aerosols: Sources and contribution from burning of C3 and C4 plants to organic aerosols, *Tellus B*, *1*, 1–14, doi:10.3402/tellusb.v66.20176.
Mortazavi, B., and J. P. Chanton (2004), Use of Keeling plots to determine sources of dissolved organic carbon in nearshore and open ocean systems, *Limnol. Oceanogr.*, *49*(1), 102–108, doi:10.4319/lo.2004.49.1.0102.
Mouteva, G. O., S. Fahrni, G. M. Sanots, J. T. Randerson, Y. L. Zhang, S. Szidat, and C. I. Czimczik (2015), Accuracy and precision of 14C-based source apportionment of organic and elemental carbon in aerosols using the Swiss_4S protocol, *Atmos. Meas. Tech.*, *8*, 3729–3743.
Myhre, G., et al. (2013), Anthropogenic and natural radiative forcing, in *Climate Change 2013: The Physical Science Basis. Contribution of Working Group I to the Fifth Assessment Report of the Intergovernmental Panel on Climate Change*, edited by T. F. Stocker et al., pp. 659–740, Cambridge Univ. Press, Cambridge, U. K., and New York, doi:10.1017/CBO9781107415324.018.
Nehrkorn, T., J. Eluszkiewicz, S. C. Wofsy, J. C. Lin, C. Gerbig, M. Longo, and S. Freitas (2010), Coupled weather research and forecasting–stochastic time-inverted lagrangian transport (WRF–STILT) model, *Meteorol. Atmos. Phys.*, *107*(1–2), 51–64.
Nier, A. O. (1950), A redetermination of the relative abundances of the isotopes of carbon, nitrogen, oxygen, argon, and potassium, *Phys. Rev.*, *77*(6), 789–793, doi:10.1103/PhysRev.77.789.
Nydal, R., and K. Lövseth (1983), Tracing bomb 14C in the atmosphere 1962–1980, *J. Geophys. Res.*, *88*(C6), 3621–3642, doi:10.1029/JC088iC06p03621.
Oris, F., H. Asselin, A. A. Ali, W. Finsinger, and Y. Bergeron (2014), Effect of increased fire activity on global warming in the boreal forest, *Environ. Rev.*, *14*, 1–14.
Palmer, P. I., et al. (2013), Quantifying the impact of BOReal forest fires on Tropospheric oxidants over the Atlantic using Aircraft and Satellites (BORTAS) experiment: Design, execution and science overview, *Atmos. Chem. Phys.*, *13*(13), 6239–6261, doi:10.5194/acp-13-6239-2013.
Pataki, D. E. (2003), The application and interpretation of Keeling plots in terrestrial carbon cycle research, *Global Biogeochem. Cycles*, *17*(1), 1022, doi:10.1029/2001GB001850.
Pavuluri, C. M., K. Kawamura, E. Tachibana, and T. Swaminathan (2010), Elevated nitrogen isotope ratios of tropical Indian aerosols from Chennai: Implication for the origins of aerosol nitrogen in South and Southeast Asia, *Atmos. Environ.*, *44*(29), 3597–3604, doi:10.1016/j.atmosenv.2010.05.039.
Pavuluri, C. M., K. Kawamura, and T. Swaminathan (2015), Time-resolved distributions of bulk parameters, diacids, ketoacids and α-dicarbonyls and stable carbon and nitrogen isotope ratios of TC and TN in tropical Indian aerosols: Influence of land/sea breeze and secondary processes, *Atmos. Res.*, *153*, 188–199, doi:10.1016/j.atmosres.2014.08.011.
Penner, J. (1995), Carbonaceous aerosols influencing atmospheric radiation: Black and organic carbon, in *Aerosol Forcing of Climate: Report of the Dahlem Workshop on Aerosol Forcing of Climate, Berlin 1994, April 24–29*, edited by R. J. Charlston and J. Heintzenberg, pp. 91–108, J. Wiley, Chichester, New York.
Penner, J. E., M. J. Prather, I. S. A. Isaksen, J. S. Fuglestvedt, Z. Klimont, and D. S. Stevenson (2010), Short-lived uncertainty?, *Nat. Geosci.*, *3*(9), 587–588, doi:10.1038/ngeo932.
Quinn, P. K., et al. (2008), Short-lived pollutants in the Arctic: Their climate impact and possible mitigation strategies, *Atmos. Chem. Phys.*, *8*(6), 1723–1735, doi:10.5194/acp-8-1723-2008.
Ramanathan, V., and G. Carmichael (2008), Global and regional climate changes due to black carbon, *Nat. Geosci.*, *1*, 221–227.
Randerson, J. T., et al. (2006), The impact of boreal forest fire on climate warming, *Science*, *314*(5802), 1130–1132, doi:10.1126/science.1132075.
Reddy, C. M., A. Pearson, L. Xu, A. P. McNichol, B. A. Benner, S. A. Wise, G. A. Klouda, L. A. Currie, and T. I. Eglinton (2002), Radiocarbon as a tool to apportion the sources of polycyclic aromatic hydrocarbons and black carbon in environmental samples, *Environ. Sci. Technol.*, *36*(8), 1774–1782.
Reid, J. S., R. Koppmann, T. F. Eck, and D. P. Eleuterio (2005), A review of biomass burning emissions, part II: Intensive physical properties of biomass burning particles, *Atmos. Chem. Phys.*, *5*, 799–825, doi:10.5194/acpd-4-5135-2004.
Rogers, B. M., S. Veraverbeke, G. Azzari, C. I. Czimczik, S. R. Holden, G. O. Mouteva, F. Sedano, K. K. Treseder, and J. T. Randerson (2014), Quantifying fire-wide carbon emissions in interior Alaska using field measurements and Landsat imagery, *J. Geophys. Res. Biogeosci.*, *119*, 1608–1629, doi:10.1002/2014JG002657.
Rogers, B. M., A. J. Soja, M. L. Goulden, and J. T. Randerson (2015), Influence of tree species on continental differences in boreal fires and climate feedbacks, *Nat. Geosci.*, *8*, 1–7, doi:10.1038/NGEO2352.
Santos, G. M., J. R. Southon, S. Griffin, S. R. Beaupre, and E. R. M. Druffel (2007), Ultra small-mass AMS ^{14}C sample preparation and analyses at KCCAMS/UCI Facility, *Nucl. Instrum. Methods Phys. Res., Sect. B*, *259*(1), 293–302, doi:10.1016/j.nimb.2007.01.172.
Schuur, E. A. G., and S. E. Trumbore (2006), Partitioning sources of soil respiration in boreal black spruce forest using radiocarbon, *Global Change Biol.*, *12*(2), 165–176, doi:10.1111/j.1365-2486.2005.01066.x.
Sharma, S. (2004), Long-term trends of the black carbon concentrations in the Canadian Arctic, *J. Geophys. Res.*, *109*, D15203, doi:10.1029/2003JD004331.
Sheesley, R. J., M. Kruså, P. Krecl, C. Johansson, and Ö. Gustafsson (2009), Source apportionment of elevated wintertime PAHs by compound-specific radiocarbon analysis, *Atmos. Chem. Phys.*, *9*, 3347–3356, doi:10.5194/acp-9-3347-2009.

Skeie, R. B., T. Berntsen, G. Myhre, C. A. Pedersen, J. Ström, S. Gerland, and J. A. Ogren (2011), Black carbon in the atmosphere and snow, from pre-industrial times until present, *Atmos. Chem. Phys.*, *11*(14), 6809–6836, doi:10.5194/acp-11-6809-2011.

Slater, J. F., L. A. Currie, J. E. Dibb, and B. A. Benner (2002), Distinguishing the relative contribution of fossil fuel and biomass combustion aerosols deposited at Summit, Greenland through isotopic and molecular characterization of insoluble carbon, *Atmos. Environ.*, *36*, 4463–4477, doi:10.1016/S1352-2310(02)00402-8.

Soja, A. J. (2004), Estimating fire emissions and disparities in boreal Siberia (1998–2002), *J. Geophys. Res.*, *109*, D14S06, doi:10.1029/2004JD004570.

Spracklen, D. V., B. Bonn, and K. S. Carslaw (2008), Boreal forests, aerosols and the impacts on clouds and climate, *Philos. Trans. R. Soc., A*, *366*, 4613–4626, doi:10.1098/rsta.2008.0201.

Stohl, A., et al. (2006), Pan-Arctic enhancements of light absorbing aerosol concentrations due to North American boreal forest fires during summer 2004, *J. Geophys. Res.*, *111*, D22214, doi:10.1029/2006JD007216.

Stohl, A., Z. Klimont, S. Eckhardt, K. Kupiainen, V. P. Shevchenko, V. M. Kopeikin, and A. N. Novigatsky (2013), Black carbon in the Arctic: The underestimated role of gas flaring and residential combustion emissions, *Atmos. Chem. Phys.*, *13*(17), 8833–8855, doi:10.5194/acp-13-8833-2013.

Stone, R. S., G. P. Anderson, E. P. Shettle, E. Andrews, K. Loukachine, E. G. Dutton, C. Schaaf, and M. O. Roman (2008), Radiative impact of boreal smoke in the Arctic: Observed and modeled, *J. Geophys. Res.*, *113*, D14S16, doi:10.1029/2007JD009657.

Stuiver, M., and H. Polach (1977), Discussion: Reporting of ^{14}C data, *Radiocarbon*, *19*(3), 355–363.

Suess, H. E. (1955), Radiocarbon concentration in modern wood, *Science*, *122*(3166), 415–417, doi:10.1126/science.122.3166.415-a.

Szidat, S., T. M. Jenk, H.-A. Synal, M. Kalberer, L. Wacker, I. Hajdas, A. Kasper-Giebl, and U. Baltensperger (2006), Contributions of fossil fuel, biomass-burning, and biogenic emissions to carbonaceous aerosols in Zurich as traced by ^{14}C, *J. Geophys. Res.*, *111*, D07206, doi:10.1029/2005JD006590.

Szidat, S., M. Ruff, N. Perron, L. Wacker, H.-A. Synal, M. Hallquist, A. S. Shannigrahi, K. E. Yttri, C. Dye, and D. Simpson (2009), Fossil and non-fossil sources of organic carbon (OC) and elemental carbon (EC) in Göteborg, Sweden, *Atmos. Chem. Phys.*, *9*, 1521–1535.

Telegadas, K. (1971), The seasonal atmospheric distribution and inventories of excess carbon-14 from March 1955 to July 1969, *Rep. HASL*, *243*, 12–187.

Tosca, M. G., D. J. Diner, M. J. Garay, and O. V. Kalashnikova (2014), Observational evidence of fire-driven reduction of cloud, *J. Geophys. Res. Atmos.*, *119*, 8418–8432, doi:10.1002/2014JD021759.

Trumbore, S. (2000), Age of soil organic matter and soil respiration: Radiocarbon constrains on belowground C dynamics, *Ecol. Appl.*, *10*(2), 399–411.

Trumbore, S. E., and J. W. Harden (1997), Accumulation and turnover of carbon in organic and mineral soils of the BOREAS northern study area, *J. Geophys. Res.*, *102*, 28,817, doi:10.1029/97JD02231.

Turekian, V. C., S. Macko, D. Ballentine, R. J. Swap, and M. Garstang (1998), Causes of bulk carbon and nitrogen isotopic fractionations in the products of vegetation burns: Laboratory studies, *Chem. Geol.*, *152*(1–2), 181–192, doi:10.1016/S0009-2541(98)00105-3.

Turetsky, M. R., E. S. Kane, J. W. Harden, R. D. Ottmar, K. L. Manies, E. Hoy, and E. S. Kasischke (2010), Recent acceleration of biomass burning and carbon losses in Alaskan forests and peatlands, *Nat. Geosci.*, *4*(1), 27–31, doi:10.1038/ngeo1027.

Turetsky, M. R., W. F. Donahue, and B. W. Benscoter (2011), Experimental drying intensifies burning and carbon losses in a northern peatland, *Nat. Commun.*, *2*, 514, doi:10.1038/ncomms1523.

Turquety, S., et al. (2007), Inventory of boreal fire emissions for North America in 2004: Importance of peat burning and pyroconvective injection, *J. Geophys. Res.*, *112*, D12S03, doi:10.1029/2006JD007281.

Val Martin, M., J. A. Logan, D. Kahn, F. Y. Leung, D. Nelson, and D. Diner (2010), Smoke injection heights from fires in North America: Analysis of 5 years of satellite observations, *Atmos. Chem. Phys.*, *10*, 1491–1510, doi:10.5194/acp-10-1491-2010.

Veraverbeke, S., B. M. Rogers, and J. T. Randerson (2015), Daily burned area and carbon emissions from boreal fires in Alaska, *Biogeosciences*, *12*, 3579–3601, doi:10.5194/bg-12-3579-2015.

Vignati, E., M. Karl, and M. Krol (2010), Sources of uncertainties in modelling black carbon at the global scale, *Atmos. Chem. Phys.*, *2*, 2595–2611.

Wang, Q., et al. (2011), Sources of carbonaceous aerosols and deposited black carbon in the Arctic in winter-spring: Implications for radiative forcing, *Atmos. Chem. Phys.*, *11*(23), 12,453–12,473, doi:10.5194/acp-11-12453-2011.

Ward, D. S., S. Kloster, N. M. Mahowald, B. M. Rogers, J. T. Randerson, and P. G. Hess (2012), The changing radiative forcing of fires: Global model estimates for past, present and future, *Atmos. Chem. Phys.*, *12*(22), 10,857–10,886, doi:10.5194/acp-12-10857-2012.

Warneke, C., et al. (2009), Biomass burning in Siberia and Kazakhstan as an important source for haze over the Alaskan Arctic in April 2008, *Geophys. Res. Lett.*, *36*, L02813, doi:10.1029/2008GL036194.

Widory, D. (2007), Nitrogen isotopes: Tracers of origin and processes affecting PM10 in the atmosphere of Paris, *Atmos. Environ.*, *41*(11), 2382–2390, doi:10.1016/j.atmosenv.2006.11.009.

Wiscombe, W., and S. Warren (1980), A model for the spectral albedo of snow, I: Pure snow, *J. Atmos. Sci.*, *37*, 2712–2732.

Xian, P., J. S. Reid, J. F. Turk, E. J. Hyer, and D. L. Westphal (2009), Impact of modeled versus satellite measured tropical precipitation on regional smoke optical thickness in an aerosol transport model, *Geophys. Res. Lett.*, *36*, L16805, doi:10.1029/2009GL038823.

Xu, X., S. E. Trumbore, S. Zheng, J. R. Southon, K. E. McDuffee, M. Luttgen, and J. C. Liu (2007), Modifying a sealed tube zinc reduction method for preparation of AMS graphite targets: Reducing background and attaining high precision, *Nucl. Instrum. Methods Phys. Res., Sect. B*, *259*(1), 320–329, doi:10.1016/j.nimb.2007.01.175.

Yokelson, R. J., et al. (2013), Coupling field and laboratory measurements to estimate the emission factors of identified and unidentified trace gases for prescribed fires, *Atmos. Chem. Phys.*, *13*(1), 89–116, doi:10.5194/acp-13-89-2013.

Yttri, K. E., et al. (2011), Source apportionment of the summer time carbonaceous aerosol at Nordic rural background sites, *Atmos. Chem. Phys.*, *11*, 13,339–13,357, doi:10.5194/acp-11-13339-2011.

Yttri, K. E., C. Lund Myhre, S. Eckhardt, M. Fiebig, C. Dye, D. Hirdman, J. Ström, Z. Klimont, and A. Stohl (2014), Quantifying black carbon from biomass burning by means of levoglucosan—A one-year time series at the Arctic observatory Zeppelin, *Atmos. Chem. Phys.*, *14*, 6427–6442, doi:10.5194/acp-14-6427-2014.

Zencak, Z., M. Elmquist, and Ö. Gustafsson (2007), Quantification and radiocarbon source apportionment of black carbon in atmospheric aerosols using the CTO-375 method, *Atmos. Environ.*, *41*(36), 7895–7906, doi:10.1016/j.atmosenv.2007.06.006.

Zhang, Y. L., N. Perron, V. G. Ciobanu, P. Zotter, M. C. Minguillón, L. Wacker, A. S. H. Prévôt, U. Baltensperger, and S. Szidat (2012), On the isolation of OC and EC and the optimal strategy of radiocarbon-based source apportionment of carbonaceous aerosols, *Atmos. Chem. Phys.*, *12*, 10,841–10,856, doi:10.5194/acp-12-10841-2012.